ADVANCED ENERGY MATERIALS
www.advenergymat.de

Decoupled Electrochemical Water Splitting: From Fundamentals to Applications

*Patrick J. McHugh, Athanasios D. Stergiou, and Mark D. Symes**

Electrolytic water splitting to generate hydrogen and oxygen is one of the most promising ways in which to harness intermittent renewable power sources and store the energy these provide as a clean-burning and sustainable fuel. In recent years, this has led to an explosion in reports on electrochemical water splitting, most of them focused on improving the efficiency of the electrochemical reactions themselves. However, efficient generation of hydrogen and oxygen is of little use if these products cannot be kept separate and the community is now coming to realize that there are considerable challenges associated with maintaining adequate separation between H_2 and O_2 during electrolysis driven by intermittent renewable sources. Decoupled electrolysis (whereby oxygen production occurs with reduction of a suitable mediator and hydrogen production is then paired with the reoxidation of this mediator) offers a solution to many of these challenges by allowing O_2 and H_2 to be produced at different times, at different rates, and even in completely different electrochemical cells. In this review, an overview of recent progress in the field of decoupled electrolysis for water splitting is given and the potential that this approach has for enabling a range of other sustainable chemical processes is explored.

1. Introduction

1.1. Electrolysis for Storage of Renewable Energy

Currently, fossil fuels such as coal, oil, and natural gas remain the world's primary sources of energy. However, it is becoming increasingly clear that greenhouse gases (such as CO_2) that are formed during combustion of these fuels are linked to oceanic and global temperature rises,[1,2] shrinking ice sheets,[3] ocean acidification,[4] and extreme weather events.[5] As the global population continues to rise, so too does global energy demand, and hence the development of energy solutions that do not rely on fossil fuels is of great importance. Renewable energy sources, such as wind, solar, and tidal energy constitute arguably the most promising of these clean energy solutions, but suffer from the fact that they are intermittent.[6] Direct power supply from these sources therefore cannot be relied upon to satisfy instantaneous energy demands.[7] A means of storing the energy generated by these renewable sources is therefore essential if we are to depend more heavily on renewably generated power.[8]

Hydrogen (H_2) is often proposed in this context as a promising "carbon neutral" energy carrier (i.e., fuel). In such a system, renewably generated electricity is used to electrolyze water to generate hydrogen and oxygen. The oxygen may be vented to the atmosphere whilst the hydrogen is stored as a fuel. This hydrogen is then subsequently oxidized (either by combustion or in a fuel cell) to regenerate water and to release energy. Hydrogen is not a perfect fuel but it does have a number of attractive properties such as its low toxicity, ability to be transported safely over long distances via pipeline,[9] and its high energy density per unit mass (three times greater than that of gasoline).[10] Moreover, sustainably sourced hydrogen could be used to reduce CO_2 or N_2 from the atmosphere to generate carbon-neutral fuels and commodity chemicals such as hydrocarbons and ammonia. In many ways then, hydrogen can be viewed as the key to a sustainable energy cycle.

The process of water electrolysis can be considered in terms of its two half-reactions: the hydrogen evolution reaction (HER) and the oxygen evolution reaction (OER). These half-equations differ somewhat depending on the pH at which the electrolysis is carried out. At low pH, the HER and OER proceed as follows (all potentials are vs the standard hydrogen electrode, SHE)

$$2H^+ + 2e^- \rightarrow H_2 \qquad \text{HER}\,(\text{pH0}, E = 0.00\text{V}) \tag{1}$$

$$2H_2O \rightarrow O_2 + 4H^+ + 4e^- \qquad \text{OER}\,(\text{pH0}, E = 1.23\text{V}) \tag{2}$$

Whereas, under alkaline conditions, the half-reactions occur as below

$$2H_2O + 2e^- \rightarrow H_2 + 2OH^- \qquad \text{HER}\,(\text{pH14}, E = -0.83\text{V}) \tag{3}$$

$$4OH^- \rightarrow O_2 + 2H_2O + 4e^- \qquad \text{OER}\,(\text{pH14}, E = 0.40\text{V}) \tag{4}$$

P. J. McHugh, A. D. Stergiou, Dr. M. D. Symes
WestCHEM
School of Chemistry
University of Glasgow
Glasgow G12 8QQ, UK
E-mail: mark.symes@glasgow.ac.uk

The ORCID identification number(s) for the author(s) of this article can be found under https://doi.org/10.1002/aenm.202002453.

DOI: 10.1002/aenm.202002453

Hence there is a significant electrical energy requirement to drive water electrolysis. Under standard conditions, a potential difference of 1.23 V is the thermodynamic minimum required to electrolyze water. However, in order to overcome various kinetic and resistance barriers (and so to drive appreciable currents to flow for the OER and HER), additional voltage is required. This additional voltage is referred to as overpotential, which is a sum of the various additional potentials relating to concentration, ohmic resistances in the electrolyzer, and to the kinetic overpotentials for the individual HER and OER half-reactions.[11] Of these overpotentials, the overpotential requirement for the OER tends to dominate as the generation of O_2 is a kinetically demanding four-electron, four-proton process.[12,13] The OER is therefore often held to be the main kinetic bottleneck for the electrolytic generation of hydrogen from water.

1.2. Conventional and Decoupled Electrolysis

In its simplest form, water electrolysis will occur under the influence of a direct current between two electrodes in a single compartment. This crude form presents many limitations, the most deleterious of which is the lack of separation of the product gases. From Equations (1)–(4), it can be seen that two moles of hydrogen are formed for every mole of oxygen generated. These gas-evolving reactions occur simultaneously, potentially creating a highly explosive mixture.[14] Commercially, this is addressed via the use of membranes or diaphragms which separate the cell into anodic and cathodic chambers. Large scale water electrolysis at high pH is carried out using a liquid alkaline electrolyte (concentrated aqueous KOH solution), at low temperatures (293–353 K) with an asbestos diaphragm.[15] In this setting, the anodic and cathodic pressures must be carefully controlled to prevent gas permeation across the separator.[16–18] Recently, considerable progress has been made in the development of solid polymer membrane electrolyzers where an anion or proton exchange membrane (e.g., Nafion) is employed within a compressed cell stack. Though relatively expensive, these cell configurations can operate at large pressure differentials, at excellent operational current densities, and without the need for caustic electrolytes. In these cells, the product streams are kept separate as gas crossover rates across the membranes are low (although crucially even these membranes are not entirely gas impermeable).[15,18–22]

The issue of separating the product gases of electrolysis becomes more complex when using renewable energy sources, where the power inputs are often variable and/or low. In such cases, the low current densities that are achieved correspond to low rates of gas production, and these rates of gas production may in turn start to approach the rates of gas crossover for some membranes, potentially leading to safety issues. A current density of 10 mA cm^{-2} is considered a useful benchmark for solar-driven electrolyzers, as this is the approximate current density expected of a water splitting device operating at 10% solar-to-fuels efficiency under "1 Sun" illumination (AM 1.5, 100 mW cm^{-2}).[23] In this scenario, crossover of hydrogen into the anodic chamber would be a real possibility and would be particularly hazardous, as the lower explosion limit of hydrogen in oxygen is only 4 mol% H_2 in O_2.[24–27] Furthermore, even if efficient and safe gas separation could be achieved, any solar-to-hydrogen device in which the half-reactions of water splitting remain coupled (as in a conventional electrolyzer, see **Figure 1**) will suffer from the fact that the rate of the relatively facile HER would still be limited by the more sluggish OER. In this context, harnessing low pressures of hydrogen gas safely and efficiently from large solar-to-hydrogen arrays is nontrivial and remains an unsolved challenge.

To this end, recent advances have been made to "decouple" these processes using redox mediators. In simple terms, a mediator with an appropriate redox potential can be employed such that the OER is coupled with the reduction of the mediator, rather than the direct generation of hydrogen. Likewise, the HER can be performed independently of the OER, by coupling hydrogen generation to the reoxidation of the mediator, rather than to water oxidation (Figure 1). With each half-reaction occurring separately, the HER can be carried out at much improved rates compared to that possible in conventional water electrolysis. In addition, the ability to perform the HER and OER both in different spaces ("spatial separation") and at different times ("temporal separation") greatly increases flexibility for harvesting hydrogen effectively and safely and significantly reduces the need for any gas purification steps. The properties required of an appropriate mediator are stability in both the oxidized and reduced forms and a reversible redox couple with a potential that resides between the onset potentials of the OER and HER. In line with the above description, decoupled electrolysis can be defined as any process where the ultimate anodic and cathodic products of electrolysis are generated under at least one of the

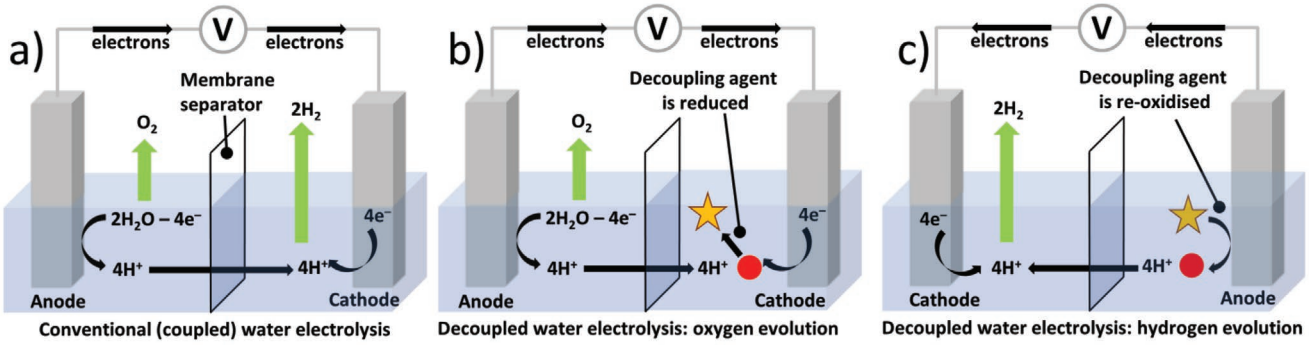

Figure 1. A comparison of a) conventional versus b,c) decoupled water electrolysis under general acidic conditions.

following conditions: i) at rates that are not intrinsically linked to each other, ii) at different times to each other, or iii) in entirely different electrochemical cells to each other.

Since its inception in 2013,[28] the field of decoupled electrolysis has advanced quickly. However, to the authors' knowledge, only three short reviews have been dedicated to the subject to date; the first being a brief perspective by Wallace and Symes,[29] the second being a short section in larger overview on water electrolysis by You and Sun,[30] and the third a minireview by Liu et al.[31] This area of research is fast moving, and none of the aforementioned papers covers any of the literature from 2019 or 2020 to any significant degree. In this review, therefore, we aim to provide a comprehensive and up-to-date assessment of this exciting and rapidly developing field as it stands at time of writing, highlighting the opportunities for decoupled electrolysis in energy storage, energy conversion, and chemical synthesis.

2. Polyoxometalate Decoupling Agents

2.1. Phosphomolybdic Acid

In 2013, Symes and Cronin introduced the concept of decoupled electrolysis using the polyoxometalate phosphomolybdic acid ($H_3PMo_{12}O_{40}$).[28,32] This polyoxometalate (a water-soluble cluster of 12 molybdenum centers held together by a central phosphate anion and numerous oxygen ligands) was used in one compartment of a two compartment cell, with the two halves of the cell being separated by a semipermeable membrane (see **Figure 2**). Decoupled water electrolysis was then achieved according to Equations (5) and (6). First, anodic water oxidation was performed yielding, O_2, protons, and electrons. However, instead of these protons and electrons combining to give hydrogen at the cathode, the counter electrode reaction was instead the reduction and protonation of the polyoxometalate (Equation (5)). This reduced and protonated polyoxometalate could be subsequently reoxidized, yielding electrons and protons which then formed hydrogen at the cathode (Equation (6)). As the reduced and protonated polyoxometalate was stable with respect to reoxidation, it could be stored for weeks before the hydrogen evolution step was performed. Hence the OER and HER could be completely decoupled from each other in both time and space and the relative rates at which hydrogen and oxygen could be generated became coupled to the rate of reduction or reoxidation of the polyoxometalate, rather than to each other. This phosphomolybdic acid redox mediator was found to buffer the pH of the electrolyte very effectively during proton release and proton consumption in Equations (5) and (6), suggesting that the polyoxometalate was accepting both the electrons and protons from water oxidation. On account of its ability to accept both electrons and protons in this manner, the term "Electron-Coupled-Proton Buffer" (ECPB) was coined to describe this and other redox mediators with similar capabilities.

$$\mathrm{ECPB} + \mathrm{H_2O} \rightarrow [\mathrm{ECPB_{(two-electron\ reduced)}}][\mathrm{H^+}]_2 + \frac{1}{2}\mathrm{O_2} \quad (5)$$

$$[\mathrm{ECPB_{(two-electron\ reduced)}}][\mathrm{H^+}]_2 \rightarrow \mathrm{H_2} + \mathrm{ECPB} \quad (6)$$

At the time, certain attributes that might make for effective Electron-Coupled-Proton Buffers were stipulated. These attributes are perhaps best viewed as guidelines, rather than rigid requirements, and indeed, it is fascinating to see how numerous successful decoupling strategies have since been developed that flout one (or more) of these attributes. For example, it was originally proposed that useful decoupling agents would display high solubility in water. However, the subsequent development of solid state decoupling agents (vide infra) shows that water solubility is not a strict requirement. Likewise, an ability to buffer the pH effectively during water splitting would seem to be important for large-scale applications (e.g., to avoid pH swings which might cause materials compatibility issues), but nevertheless examples of nonbuffering decoupling agents have also been demonstrated (at least on the lab-scale). Others of the original guidelines remain (as yet) unchallenged: the requirement that the decoupling agent should have at least one reversible redox couple which falls between the onset potentials of the HER and OER, and that it should be stable in both the oxidized and reduced forms (in order to allow both the oxygen and hydrogen evolution steps to be performed in a controlled manner) seem to be common features of the decoupling agents

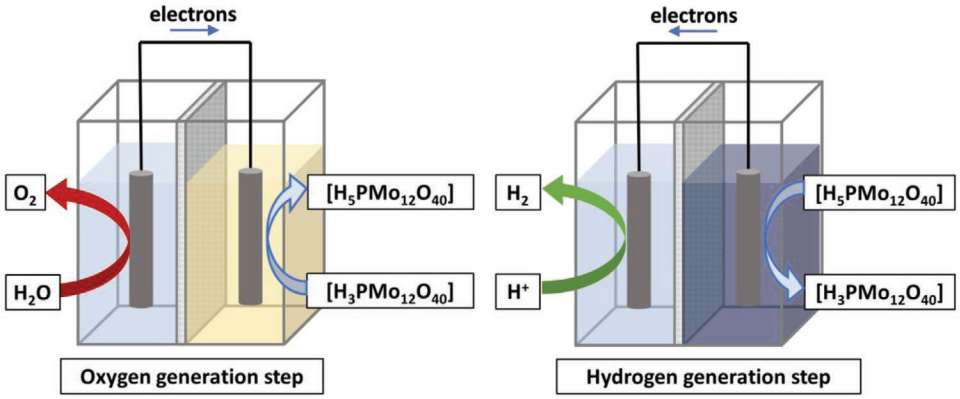

Figure 2. Decoupled water electrolysis using phosphomolybdic acid as the decoupling agent. Left: The oxygen evolution step where water oxidation is coupled with the reduction of phosphomolybdic acid, which undergoes a color change from yellow to dark blue as it accepts electrons and protons. Right: The subsequent hydrogen evolution step, where the phosphomolybdic acid is reoxidized.

that will be discussed in this review. It is also generally desirable for the decoupling agent to consist only of abundant, low-cost elements and for its synthesis to be straightforward.

In this context, phosphomolybdic acid makes a very good choice as a mobile (i.e., able to be pumped or flowed around a continuously operating system) decoupling agent and Electron-Coupled-Proton Buffer. It has a number of suitably positioned redox waves,[33] is commercially available, and can be prepared at concentrations in excess of 0.5 M simply by dissolving the solid in water at room temperature. It buffers the pH extremely well during both the water oxidation and hydrogen evolution processes as it converts between the fully oxidized ($H_3PMo_{12}O_{40}$) and two-electron-reduced ($H_5PMo_{12}O_{40}$) forms and it is stable in solution in both these forms (including with respect to reoxidation by air in the case of $H_5PMo_{12}O_{40}$) for many weeks. When used as an Electron-Coupled-Proton Buffer for decoupled electrolysis of water, phosphomolybdic acid allows complete separation of oxygen and hydrogen generation in a stable and cyclable fashion, and therefore forms a useful benchmark against which to assess the decoupling agents and decoupling strategies that have been reported since. **Table 1** gives a summary of some of the key metrics of the decoupling agents for water splitting that are discussed in this review.

One of the key claims made for decoupled electrolysis is that it may enable more practical device designs for solar-to-hydrogen systems when compared to the concept of vast, flat arrays producing hydrogen and oxygen on either side of a gas-permeable membrane at a rate limited by the rather low power provided by solar irradiation. Indeed, the challenges of harvesting low-pressure hydrogen from such a large array are considerable, even in the absence of any oxygen crossover from the anodic chamber into the hydrogen to be harvested. The first

Table 1. Some key metrics of the decoupling agents for water splitting discussed in this review.

Mediator	Redox Potential (V vs SHE)	pH for Redox Potential	No. of Cycles Tested	Best Reported Faradaic Efficiency (HER)	Best Reported Faradaic Efficiency (OER)	References
$H_3PMo_{12}O_{40}$	+0.50, +0.65	0.3	5	100%	100%	Symes and Cronin[28] Bloor et al.[34] Li et al.[38]
$H_4[SiW_{12}O_{40}]$	0.0, –0.22	0.5	9	95 ± 7%	100%	Rausch et al.[43] Chisholm et al.[44] Wu et al.[85]
$H_3PW_{12}O_{40}$	+0.237, –0.036	0.42	–	44.6%	–	Macdonald et al.[46]
$H_4SiO_4{\cdot}12MoO_3$	+0.509	0.69	–	–	–	Macdonald et al.[46]
$H_6ZnW_{12}O_{40}$	–0.078 –0.198	0.4	200	95.5%	–	Lei et al.[49]
$[P_2W_{18}O_{62}]^{6-}$	+0.3, +0.1, 0 to –0.5	1	100	–	–	Chen et al.[50]
V(III)/V(II)	–0.26	0	–	96 ± 4%	–	Amstutz et al.[51] Ho et al.[53]
Ce(IV)/Ce(III)	+1.48	0	–	–	78 ± 8%	Amstutz et al.[51]
$Fe(CN)_6^{3-}/Fe(CN)_6^{4-}$	+0.77	7.2	–	99.88%	–	Goodwin and Walsh[55] Ma et al.[86]
FcNCl	+0.6	6.5	20	100%	100%	Li et al.[56]
Hydroquinone sulfonate	+0.65	0.7	20	98 ± 7%	91 ± 5%	Rausch et al.[61]
AQDS	+0.214	0	100	100%	100%	Kirkaldy et al.[62]
$NiOOH/Ni(OH)_2$	+0.55	14	100	100%	100%	Chen et al.[64] Landman et al.[66,74] Dotan et al.[72]
FeO_x	+0.8 to +1.5	14	50	>90%	>90%	Jin et al.[75]
$MnO_2/MnOOH$	+0.15	14	10	≈100%	–	Choi et al.[76]
$Fe_3O_4/FeOOH$	–	–	–	100%	–	Palumbo et al.[77]
CoO	–	–	–	100%	–	Nudehi et al.[78]
PTPAn	+0.789 +0.689	0.3	120	97.8%	97.8%	Ma et al.[79]
PTO	+0.46 +0.589	0.3	300	98.7%	98.7%	Ma et al.[83]
PANI	+0.45 +0.91	0.3	40	–	–	Wang et al.[84]

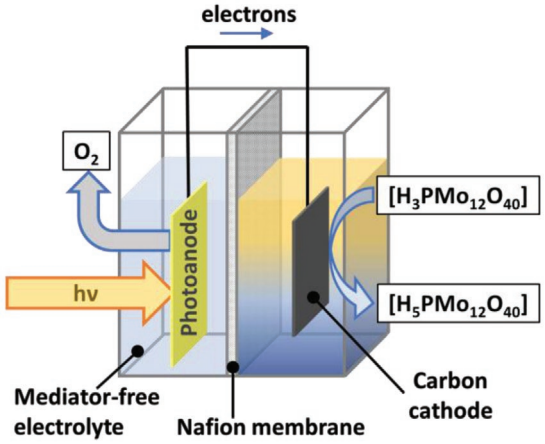

Figure 3. The photoelectrochemical cell developed by Bloor et al.[34] for the reduction of phosphomolybdic acid at a carbon cathode powered solely by visible light irradiation of a WO_3 photoanode.

steps in showcasing decoupling as a way around some of these technical challenges were taken by Bloor et al., again using phosphomolybdic acid as the decoupling agent.[34] In that study, a tungsten trioxide (WO_3) photoanode was employed to perform water oxidation within a photoelectrochemical cell, where the cathode reaction was reduction and protonation of phosphomolybdic acid (Equation (5)), rather than direct hydrogen production (see **Figure 3**). The choice of WO_3 (on a fluorine-doped tin oxide substrate) as the photoanode was dictated by its good stability in acidic electrolytes and for its reasonable (if perhaps unspectacular) visible light absorption properties. In undoped form, WO_3 has a well-positioned valance band edge for the oxidation of water at low pH, but the position of its conduction band is insufficiently reductive to allow WO_3 to drive the reduction of protons to hydrogen concomitant with water oxidation.[35] However, photoanodes using WO_3 should have the ability to drive water oxidation at the anode coupled to the simultaneous reduction of phosphomolybdic acid at the cathode, on account of phosphomolybdic acid's more positive redox potential than hydrogen (around +0.65 V vs SHE at pH 0.5). Hence in the absence of phosphomolybdic acid, no photocurrent was recorded in a setup similar to that shown in Figure 3. However, upon illumination with AM 1.5 light at 1 Sun intensity, photocurrents in excess of 1 mA cm^{-2} could be achieved for oxygen generation at the WO_3 photoanode (coupled to phosphomolybdic acid reduction at the cathode) with no external potential bias. These current densities for the photocatalytic water oxidation process compared favorably with photocurrents obtained at low pH (but using applied biases) in other studies using WO_3 photoanodes.[36,37] Importantly, no hydrogen production took place during this photodriven water oxidation and phosphomolybdic acid reduction process, eliminating any concerns about gas crossover. As the reduced decoupling agent is stable with respect to spontaneous reoxidation, there is, therefore, the potential to trickle-charge the polyoxometalate solution at low current densities as oxygen is slowly evolved at the photoanode and allowed to vent to the atmosphere. The reduced polyoxometalate solution (once a desired level of reduction has been reached) could then be pumped to a separate hydrogen-evolving cell where it could be reoxidized at high current density, liberating hydrogen at the cathode for compression and storage. The generation of hydrogen at such a point-source electrolyzer, remote from the light harvesting array, would dramatically increase the efficiency and safety of hydrogen collection. Further economies could be realized by combining multiple polyoxometalate-reducing photoarrays with a single polyoxometalate reoxidation cell in order to maximize any expensive components (e.g., hydrogen evolution electrocatalysts) used in this hydrogen generation cell.

A similar concept using phosphomolybdic acid as a decoupling agent in a light-driven scheme has been proposed by Li et al.[38] In their setup, oxygen evolution was achieved upon irradiation of mixtures containing a powder of the n-type semiconductor bismuth vanadate ($BiVO_4$) and phosphomolybdic acid. As with WO_3, the bandgap of $BiVO_4$ is well positioned to facilitate water oxidation and concomitant phosphomolybdic acid reduction.[39,40] After irradiation, the reaction mixture was transferred to a two-compartment cell where, using Pt mesh working and Pt wire counter electrodes, the reduced phosphomolybdic acid formed in the photolytic step was reoxidized with corresponding hydrogen evolution at the cathode. The Faradaic efficiency of the HER using this method was found to be 98%. Suspensions of other, well established n-type semiconductors, such as Ag_3PO_4 and Fe_2O_3, were also assessed for use by this method; it was found that none were as efficient as $BiVO_4$. One issue encountered by the authors, as their semiconductor was mixed into their mediator solution, was that the characteristic color change of phosphomolybdic acid from yellow to dark blue which occurs upon its reduction inhibited the absorption of light by the semiconductor. Increasing the transparency of solutions of phosphomolybdic acid was listed as future work that might increase the efficiency of the decoupled photolytic water oxidation step. In this regard, it is useful to note that in the setup described by Bloor et al., the polyoxometalate is confined to the cathode compartment of the photoelectrochemical cell, whilst the semiconductor is confined to the anode, and hence the polyoxometalate does not attenuate the light reaching the photoanode.[34]

An interesting aside can be made at this point to consider the activity of phosphomolybdic acid and certain vanadium-substituted phosphomolybdates as decoupling agents in hydrogen/oxygen fuel cells (i.e., performing the reverse reaction to electrochemical water splitting). Building on preliminary data reported by Shah and co-workers,[41] Matsui et al. studied the effectiveness of a range of phosphomolybdates of the general formula $H_{3+x}PV_xMo_{12-x}O_{40}$ ($x = 0$, 2, and 3) in terms of their ability to be reduced by hydrogen and then subsequently oxidized by O_2.[42] The concept (**Figure 4**) relies on the oxidation of H_2 gas at the Pt/C anode of a proton exchange membrane fuel cell to generate protons and electrons. In a conventional proton exchange membrane fuel cell, these protons and electrons would combine with O_2 at the cathode side of the cell to generate water, releasing energy in the process. However, significant amounts of Pt are required at the cathode to perform this oxygen reduction reaction and the kinetics of oxygen reduction constitute a significant bottleneck. By using a decoupled approach, Matsui et al. replaced the direct oxygen reduction reaction with reduction and protonation of their phosphomolybdate ions, which

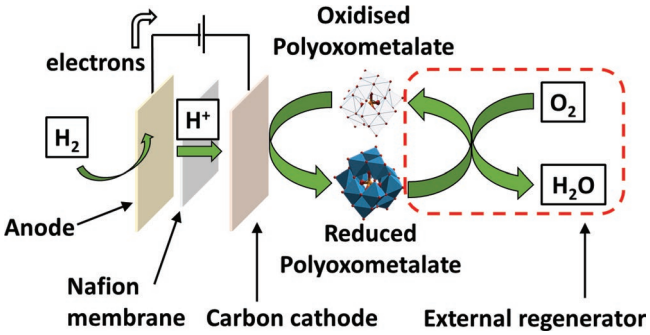

Figure 4. A decoupled proton exchange membrane hydrogen/oxygen fuel cell using a liquid polyoxometalate-based decoupling agent.

occurred at a purely carbon cathode. The reduced and protonated polyoxometalate solution was then flowed into a "regenerator," where bubbling with O_2 caused the polyoxometalate to be oxidized back to its original form (with cogeneration of water) for return to the fuel cell. In this way, the sluggish electrochemical oxygen reduction reaction could be decoupled from the hydrogen oxidation reaction, with the ultimate water-producing step taking place outside the electrochemical cell in a nonelectrochemical step. Temperature and pH were found to be crucial factors for the optimization of the fuel cell. The optimal conditions found to be 80 °C and a basic pH achieved by employing an equimolar ratio of sodium carbonate to polyoxometalate. Under these conditions, the system was able to generate a stable current density of 5.36 mA cm^{-2} at a terminal voltage of about 0.7 V over the course of an hour. This approach shows considerable promise for the development of new fuel cell systems where Pt use is minimized and where current flow (and hence power generation) can be optimized by decoupling the electrochemical oxygen reduction reaction from the oxidation of the hydrogen fuel.

2.2. Silicotungstic Acid

Decoupling the OER and HER from each other comes at an energetic cost. This is because the decoupling agent must be reduced as the OER takes place and then reoxidized as the HER occurs. If these steps are performed electrochemically, then there are two additional sets of overpotential requirements for the decoupling agent's reduction and reoxidation over and above those required for the OER and HER. In their original decoupling paper, Symes and Cronin estimated that at a current density of 100 mA cm^{-2}, their decoupled system was only 87% as efficient as the analogous direct water splitting process in a coupled arrangement.[28] Hence, strategies that minimize the number of additional electrochemical processes should help to increase the efficiency of decoupled electrolysis.

To this end, Rausch et al. explored the use of silicotungstic acid ($H_4[SiW_{12}O_{40}]$) as an alternative polyoxometalate-based decoupling agent.[43] Compared to phosphomolybdic acid, the first two redox waves of silicotungstic acid are significantly more cathodic, with $E_{1/2}$ values of +0.01 and –0.22 V (vs SHE) at pH 0.5. The position of this second wave in particular has significant implications for silicotungstic acid's activity as a decoupling agent. On a carbon electrode, both of these reduction reactions occur at considerably more positive potentials than proton reduction (the current density for which is not appreciable at potentials more positive than –0.6 V vs SHE). This means that at a carbon cathode, it should be possible to reduce silicotungstic acid by two electrons without any competing hydrogen evolution. However, as the redox potentials suggest, the two-electron-reduced silicotungstic acid is thermodynamically unstable with respect to reoxidized polyoxometalate and hydrogen evolution and so should spontaneously reoxidize (generating hydrogen at the same time) when in contact with a suitable catalyst, without the need for any additional electrochemical bias. This would eliminate the need for an electrochemical polyoxometalate reoxidation/hydrogen evolution step and hence make decoupling more effective.

To illustrate this concept, Rausch et al. electrolyzed water at a Pt mesh anode in a two-compartment cell, whilst silicotungstic acid was reduced at a carbon cathode in the other chamber (**Figure 5**). Gas chromatography indicated a 100% Faradaic efficiency for oxygen evolution under these conditions, with only trace amounts of hydrogen being detected in the electrochemical cell. Decoupling of the OER and HER was therefore highly effective. Electrolysis was continued until all the silicotungstic acid had been reduced by two electrons, generating species akin to $H_6[SiW_{12}O_{40}]$. This two-electron-reduced decoupling agent was then removed from the electrochemical cell and exposed to various catalysts in order to generate hydrogen spontaneously. MoS_2 and Ni_2P were both found to be effective, but the best results in terms of depth of reoxidation and speed of hydrogen generation were obtained using Pt on a carbon support. Indeed, per milligram of Pt used, the rate of hydrogen produced from this decoupled system was 30 times faster than for a state-of-the-art proton exchange membrane electrolyzer, which is attributable to the fact that the Pt/C catalyst in the decoupled system does not require an electrical connection and so can be used in a 3D configuration, whilst in an electrolyzer the Pt/C electrocatalyst must be in contact with a current collector and hence is confined to a less catalytically optimal 2D plane.

In terms of electrochemical efficiency, some of the improvements relative to coupled electrolysis that it was hypothesized would be possible also seem to have been borne out: at a current density of 50 mA cm^{-2}, the decoupled system using

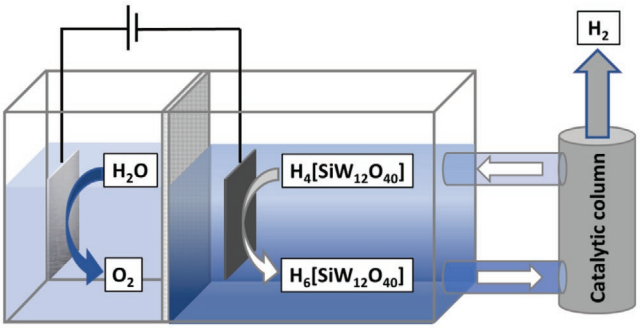

Figure 5. The silicotungstic acid-mediated system reported by Rausch et al.[43] Oxygen is produced via water oxidation alongside reduction of the mediator to $H_6[SiW_{12}O_{40}]$. Subsequent hydrogen production is achieved spontaneously in a separate chamber upon introduction of a suitable catalyst, regenerating $H_4[SiW_{12}O_{40}]$.

silicotungstic acid as a mediator was found to be 16% more efficient than a coupled electrolysis system making oxygen and hydrogen at the same time on a Pt anode and carbon cathode, respectively.

As suggested by the relative positions of the first redox wave of silicotungstic acid (+0.01 V vs SHE at pH 0.5) and the position of hydrogen evolution onset on Pt at this pH (≈–0.03 V), the spontaneous reoxidation of reduced silicotungstic acid on a Pt catalyst reaches an equilibrium whereby the decoupling agent exists as a mixture of completely reoxidized $H_4[SiW_{12}O_{40}]$ and one-electron-reduced $H_5[SiW_{12}O_{40}]$. Hence on the first usage of silicotungstic acid as a decoupling agent, the Faradaic efficiency for hydrogen generation is only 68%, as the polyoxometalate remains somewhat reduced after contact with the catalyst. However, in a system under continuous flow where the electrolyte is recycled, the Faradaic efficiency on subsequent runs would increase as the polyoxometalate cycles between this equilibrium position and its fully reduced $H_6[SiW_{12}O_{40}]$ form. Indeed, silicotungstic acid was found to be stable over 20 consecutive redox cycles and so was suggested to be viable for use in a continuous-flow reactor.

Recently, the performance of silicotungstic acid for use in just such a continuous flow reactor based on a proton exchange membrane electrolyzer has been assessed by Chisholm et al.[44] In that setup, the decoupled HER and OER steps were performed in two interconnected electrochemical flow cells (**Figure 6**). Both the OER and HER cells employed a Nafion-117 membrane, coated on one side with a catalyst. In the OER cell, the anodic side was coated with IrO_2, while in the HER cell the cathodic side was coated with Pt/C.

The operation of the continuous flow process was carried out as follows. In the OER cell, for both the anolyte and the catholyte, a fully oxidized solution of silicotungstic acid ($H_4[SiW_{12}O_{40}]$) in water was initially flowed through the cell. Galvanostatic electrolysis (i.e., at a fixed current density) was then carried out, with oxygen being produced at the anode, and the silicotungstic acid solution on the cathode side becoming reduced. The reduced silicotungstic acid solution was then fed from the cathode of the OER cell to the anode of the HER cell, with the circuit of the HER cell left open to prevent spontaneous reoxidation of the reduced silicotungstic acid ("charging" in Figure 6). Once a complete one-electron reduction of the silicotungstic acid in the catholyte loop of the OER cell was achieved (generating $H_5[SiW_{12}O_{40}]$), the circuit of the HER cell was closed. Galvanostatic electrolysis was then performed across both the OER and HER cells such that the rate at which $H_5[SiW_{12}O_{40}]$ was reduced to $H_6[SiW_{12}O_{40}]$ in the OER cell matched the rate at which $H_6[SiW_{12}O_{40}]$ was reoxidized to $H_5[SiW_{12}O_{40}]$ in the HER cell. In this way, the system was placed into steady state with silicotungstic acid cycling between $H_6[SiW_{12}O_{40}]$ and $H_5[SiW_{12}O_{40}]$ whilst oxygen and hydrogen were continuously produced at the anode of the OER cell and cathode of the HER cell, respectively. Strictly speaking, it should not be necessary to supply any voltage to reoxidize $H_6[SiW_{12}O_{40}]$ to $H_5[SiW_{12}O_{40}]$ in the HER cell; however, in practice the application of a voltage was found beneficial for ensuring a stable current density (and hence that steady-state was maintained).

Several key results were reported by the authors of this study. First, a comparison was made between the charge passed in initially reducing the silicotungstic acid, relative to the charge required to fully reoxidize the solution at the end of various periods of steady-state operation. This information, measured across three different operational current densities, gave an indication as to how stable the system was during steady-state. At 100, 250, and 500 mA cm^{-2}, the final reoxidation step required 105%, 93%, and 99% of the initial reduction charge, respectively, thus demonstrating that the process was indeed operating at a steady state to a high degree. Additionally, the amount of hydrogen that could be detected in the catholyte loop was recorded at these current densities. This indicated the extent to which the mediator was decoupling both half-reactions of electrochemical water splitting. Using a 0.4 M silicotungstic acid solution, at a cathodic flow rate of 500 mL min^{-1}, the authors reported decoupling percentages ≥99%.

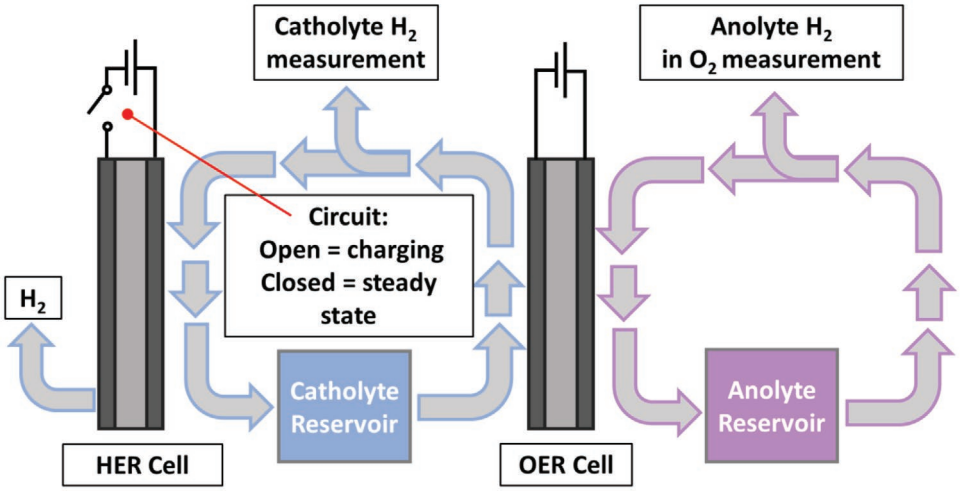

Figure 6. Schematic of the continuous flow setup used by Chisholm et al.[44] During charging, the circuit on the HER cell remains open as the silicotungstic acid in the catholyte loop is reduced, with accompanying oxygen evolution at the anode of the OER cell. To place the cell into steady state mode, the circuit on the HER cell is closed and a fixed current is applied such that the rate of reoxidation of the silicotungstic acid matches the rate of its reduction in the OER cell. Hydrogen is then generated at the cathode of the HER cell.

More impressively, crossover of hydrogen into the oxygen stream from the anode of the OER cell was found to be significantly attenuated at various rather low current densities that might better reflect operation using low power and/or intermittent renewable energy sources. Indeed, at a current density of 25 mA cm^{-2}, the decoupled system exhibited hydrogen-in-oxygen levels of only 0.31%, whereas a conventional (coupled) electrolyzer using analogous components was found to have hydrogen-in-oxygen levels of 1.9% under the same conditions. Given that guidelines for the allowable levels of hydrogen-in-oxygen put an upper limit on this figure of 0.4%,[45] the decoupled system has clear potential safety benefits over coupled systems at these low current densities.

2.3. Other Polyoxometalates

In the decoupled water electrolysis systems discussed so far, catalysis of the HER was largely performed using Pt-based catalysts. Noting the scarcity of Pt, MacDonald and co-workers investigated the performance of two molybdenum (Mo_2C and MoS_2) and two nickel phosphide (Ni_2P and Ni_5P_4) catalysts for the HER in decoupled electrolysis.[46] These authors also expanded the library of polyoxometalate decoupling agents to include phosphotungstic acid and silicomolybdic acid alongside silicotungstic acid and phosphomolybdic acid. The rationale for these choices of decoupling agents was the differing positions of their redox potentials. Accordingly, 1 M solutions of all four decoupling agents were prepared and subjected to electrochemical reduction by two electrons each. These reduced solutions were then introduced to the Mo and Ni-based catalysts and the rates and extent of hydrogen evolution from these systems were compared. In the case of silicotungstic acid and phosphotungstic acid, spontaneous hydrogen evolution was detected using all four of the catalysts, with hydrogen evolution from silicotungstic acid showing superior rates and larger yields than those achievable with phosphotungstic acid, presumably due to silicotungstic acid's more negative reduction potentials. Meanwhile, and perhaps as might have been predicted, no spontaneous hydrogen evolution was detected from reduced phosphomolybdic acid or silicomolybdic acid solutions with any catalyst (even Pt), as the redox waves for these reduced species are all more positive than that for proton reduction to hydrogen. Of the four nonprecious metal catalysts tested, the fastest rates of hydrogen evolution were recorded using Ni_5P_4 and Mo_2C, although these both generated H_2 at inferior rates relative to Pt/C.

In the examples discussed thus far, the decoupled processes have relied on (at most) two-electron reduction and reoxidation cycles of the polyoxometalate decoupling agent. However, one of the most promising features of polyoxometalates as redox mediators is that they can often reversibly accept and donate a much greater number of electrons than this.[47,48] In 2019, Lei et al. conducted a comparative study of three allied tungsten-based Keggin polyoxometalates of the form $[XW_{12}O_{40}]$ (where $X = P^{5+}$, Si^{4+}, or Zn^{2+}), in order to ascertain the effect of the central heteroatom on the redox properties of the clusters.[49] By reductive bulk electrolysis, the authors confirmed the two-electron nature of the reductions of both phosphotungstic acid and silicotungstic acid but found that the Zn^{2+} analogue, $H_6ZnW_{12}O_{40}$, was able to undergo reduction by up to four electrons under the same conditions. There was no significant change in pH during this reduction (or the subsequent electrochemical reoxidation), suggesting that $H_6ZnW_{12}O_{40}$ is an effective Electron-Coupled-Proton Buffer. When used as a decoupling agent for electrochemical water splitting, $H_6ZnW_{12}O_{40}$ exhibited excellent metrics; decoupling of the OER and HER was essentially total and over 200 cycles in a continuous flow system, the mediator showed good stability and displayed a Coulombic efficiency for each cycle well in excess of 90%.

As a final example of polyoxometalate decoupling agents for use in water splitting, we shall consider the use of the Wells–Dawson polyoxoanion $[P_2W_{18}O_{62}]^{6-}$ as reported by Chen et al. in 2018.[50] Remarkably, this polyoxometalate was found to be able to reversibly accept up to 18 electrons in aqueous solution without significant cogeneration of hydrogen, provided the concentration of the polyoxoanion exceeded 0.1 M and provided that the pH was kept below 1 (presumably, the reduced polyoxoanion is stabilized by a high proton concentration).

To investigate this polyoxometalate as a decoupling agent, the authors assembled a dual electrochemical flow cell system as shown in **Figure 7**. In one proton exchange membrane cell (the "OER cell"), water was oxidized at a controlled current density at an IrO_2 anode with concomitant reduction of $[P_2W_{18}O_{62}]^{6-}$ at the cathode. The reduced polyoxometalate then flowed to the polyoxometalate holding tank, from where it could be directed back through the OER cell in order to reduce it further. Once the polyoxoanion had been reduced to the chosen degree, the solution was then fed into the second electrochemical cell (the "HER cell") where reoxidation of the polyoxometalate could be carried out with concomitant cathodic hydrogen production from water. Comparison of the charge passed when reducing the polyoxoanion with the charge obtained upon its reoxidation indicated how reversible the charge storage process was. The authors reported that at $Li_6[P_2W_{18}O_{62}]$ concentrations of 0.1 M, 96% of the charge could be recovered, equating to around 17.2 electrons recovered for every 18-electron reduction of each polyoxoanion. The "lost" charge in this case can arise through two

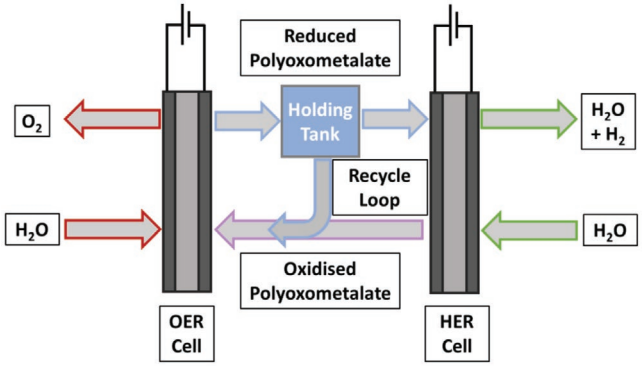

Figure 7. Schematic of the flow cell system employed by Chen et al.[50] Oxygen and hydrogen are produced separately in two proton exchange membrane cells. These reactions are decoupled by the reduction and reoxidation of $[P_2W_{18}O_{62}]^{6-}$. The polyoxometalate can be held in the holding tank and recycled to the OER cell until a desired level of reduction has been achieved.

mechanisms: i) spontaneous reoxidation of the 18-electron-reduced polyoxometalate on contact with trace oxygen in the system and ii) low levels of spontaneous hydrogen evolution from the 18-electron-reduced polyoxometalate in the presence of metallic impurities. Although reduction of the polyoxoanion was found to be possible up to a total of 32 electrons per polyoxoanion, the Coulombic efficiency based on recovered electrons decreased markedly beyond 18-electron reduction, indicating that anions of greater than this 18-electron reduction level were not stable with respect to spontaneous hydrogen evolution. In contrast, the stability of this decoupling agent under multiple successive 18-electron reduction and reoxidation cycles was found to be excellent. Over 100 cycles, the Coulombic efficiency of the reduction/reoxidation process was found to be over 95%, demonstrating the viability of this polyoxometalate cluster as an effective mediator for continuous flow decoupled water electrolysis. When the 18-electron-reduced decoupling agent was exposed to powdered Pt/C, spontaneous hydrogen evolution occurred at a rate of 3500 mmol of H_2 per hour per mg of Pt, significantly in excess of the rate of hydrogen evolution in a conventional proton exchange membrane electrolyzer (where typical values are on the order of 50–100 mmol of H_2 per hour per mg of Pt).

The ability of $[P_2W_{18}O_{62}]^{6-}$ to reversibly accept and donate such a large number of electrons prompted an investigation into its potential to act as an energy storage medium in its own right, rather than solely as a mediator for the production of hydrogen. Accordingly, a redox flow battery was constructed in which solutions of $[P_2W_{18}O_{62}]^{n-}$ served as the negative electrolyte and a mixture of HBr/Br_2 served as the positive electrolyte. At a $[P_2W_{18}O_{62}]^{n-}$ concentration of 0.5 M, a practical discharge capacity density of 230 Ah L^{-1} was achieved with a Coulombic efficiency approaching 100% and an energy density (for the polyoxometalate solution) of 225 Wh L^{-1}. This energy density is around four to five times that of currently available vanadium–vanadium redox flow batteries, suggesting that such decoupling agents could find utility in devices that can either store renewably generated energy (when operating as flow batteries) or generate hydrogen on demand, depending on the requirements of the user.

3. Transition Metal Redox Mediators

3.1. Vanadium Salts

Decoupled electrolysis systems inspired by redox flow batteries have also been developed using more conventional flow battery electrolytes. In 2014, Amstutz et al. reported a system for the decoupled electrolysis of water using a vanadium-based catholyte and cerium-based anolyte.[51] To mediate water electrolysis, a solution containing a V(III) salt in sulfuric acid was reduced to a V(II) solution at a graphite felt electrode. The position of the V(III)/V(II) redox couple (–0.26 V vs SHE under the conditions used) is negative of the proton reduction couple, and so (just as with the silicotungstic acid systems discussed above[43,44]), exposure of this V(II) solution to hydrogen evolution catalysts should give rise to spontaneous (nonelectrochemical) hydrogen generation. Hence, when this V(II) solution was directed into an external catalytic reactor, the HER occurred over an Mo_2C catalyst with a Faradaic yield of up to 96% (Equation (7) and **Figure 8**).

$$2V^{2+} + 2H^+ \rightarrow H_2 + 2V^{3+} \quad (7)$$

$$4Ce^{4+} + 2H_2O \rightarrow 4Ce^{3+} + 4H^+ + O_2 \quad (8)$$

Similarly, at the anode of the flow-battery type system, an acidic solution of Ce(III) was oxidized to Ce(IV). The position of the Ce(III)/Ce(IV) redox couple under these conditions is more anodic than that for water oxidation, meaning that (in the presence of a suitable catalyst), Ce(IV) should be able to oxidize water to generate oxygen, becoming reduced back to Ce(III) in the process (Equation (8)). In practice, Amstutz et al. achieved this catalytic water oxidation reaction over RuO_2 nanoparticles. The Faradaic yield for the OER (78% ± 8%)

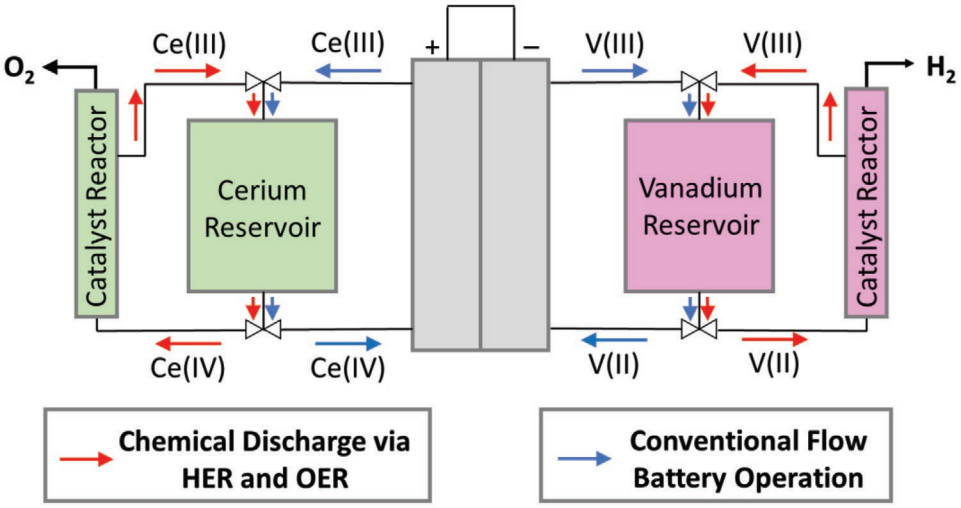

Figure 8. Schematic of the Ce-V redox flow battery system employed by Amstutz et al.[51] where valves allow for on-demand H_2 or O_2 production via routing of the electrolytes to external catalytic reactors.

was somewhat less than optimal, which was attributed to a side reaction (previously reported in the literature[52]) whereby Ce(IV) reacts with (and degrades) the RuO_2 catalyst as it is reduced back to Ce(III). The authors suggested that this issue could be avoided by adapting the electrolyte to an all-vanadium system (where the OER would then be mediated by the reduction of V(V) to V(IV)). As with the $[P_2W_{18}O_{62}]^{n-}$ system,[50] this device configuration allowed both for conventional operation as a redox flow battery (the electrolyte could be charged and discharged with electrical energy, cycling between V(II) and V(III) at one electrode and between Ce(IV) and Ce(III) at the other), and for the conversion of energy to hydrogen, offering considerable flexibility for renewable energy usage to the operator.

Ho et al. have also made use of the V(III)/V(II) redox couple in their solar-driven approach to decoupled water electrolysis.[53] The authors noted that there were numerous examples of earth-abundant OER electrocatalysts, with optimal stability when used at alkaline pH.[54] However, the V(III)/V(II) couple for HER generation is only soluble at low pH. By employing a bipolar membrane, a large pH differential between the anode and cathode compartments of their electrochemical cell could be maintained, allowing the OER side to be at high pH whilst the HER side was at very low pH (**Figure 9**). This dual electrolyte system consisted of an anodic chamber with a Ni mesh oxygen evolution electrode in concentrated KOH (2.5 M) and a cathodic chamber using a Pt foil electrode in sulfuric acid (2.0 M). At the Ni anode, OH^- was oxidized yielding electrons, water and oxygen; these electrons travelled through the external circuit to the cathode, where they reduced V(III) ions to V(II). Once charged, the V(II) solution was then transferred to a separate reactor where, when stirred with an Mo_2C catalyst, hydrogen was produced on-demand. The Faradaic efficiency of the hydrogen production step using this cell was investigated at different depths of charge of the vanadium solution: when this solution was reduced to 27%, 55%, and 96% of its charging capacity, the amount of hydrogen collected corresponded to Faradaic efficiencies of 87%, 87%, and 83%, respectively. Hydrogen generation under elevated pressures (important for compression and storage efficiencies) was also demonstrated: at pressures of up to ten atmospheres, hydrogen could be produced at Faradaic efficiencies approaching 60%.

To ascertain the extent to which the bipolar membrane would allow extended operation, the rates of ion crossover across the bipolar membrane were recorded by monitoring the vanadium salt concentrations in the anolyte, using inductively coupled plasma mass spectroscopy, after the cell was subjected to a current of 10 mA cm^{-2} for 24 h. It was determined that the current density corresponding to V(III)/V(II) leakage over this time was negligible (0.226 μA cm^{-2}), although the effects of this leakage over longer stretches of operation is yet to be determined. This test also indicated that the presence of the V(III)/V(II) species did not negatively affect the selectivity of the bipolar membrane. Furthermore, the authors demonstrated that the system could be powered directly by renewable energy by coupling it to a photovoltaic module: using only the power supplied by this photovoltaic under solar irradiation, hydrogen was produced at a Faradaic efficiency of 80% and a solar-to-hydrogen energy conversion efficiency of 5.8% was achieved. This represents a significant milestone in demonstrating the practicality of decoupled electrolysis for solar-to-hydrogen conversion.

3.2. Iron Complexes

In 2017, Goodwin and Walsh introduced a novel approach to spatially decouple the OER and HER, which made use of the $Fe(CN)_6^{3-}/Fe(CN)_6^{4-}$ redox couple and a closed bipolar electrode.[55] Bipolar electrodes are conducting components which can promote both anodic and cathodic reactions simultaneously; these electrodes are further denoted as "closed" when their poles are in two separate solutions. In their setup, Goodwin and Walsh employed two carbon cloths connected by a wire as the closed bipolar electrode, which bridged between two separate two-compartment cells (**Figure 10**). Inside each two-compartment cell, one end of the closed bipolar electrode was submerged in a solution of $K_3Fe(CN)_6/K_4Fe(CN)_6$ in 0.1 M KOH.

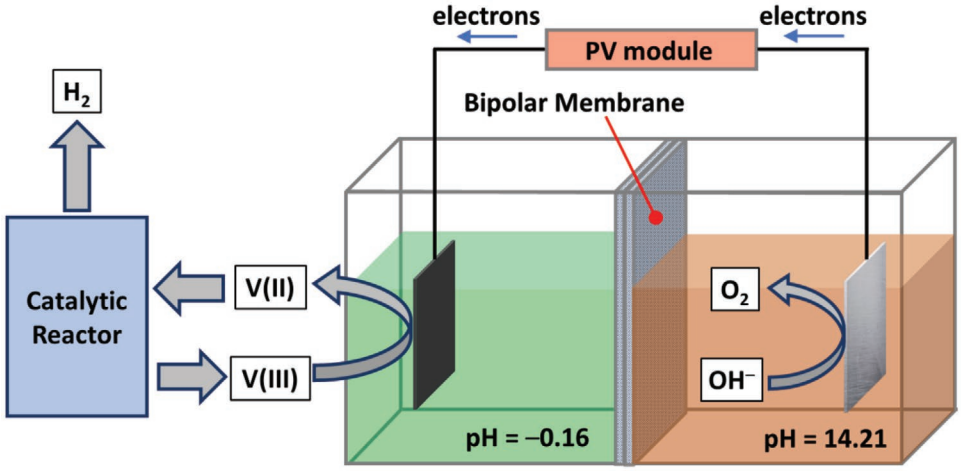

Figure 9. Diagram of the setup used by Ho et al.[53] where alkaline oxygen evolution is coupled with the reduction of V(III) to V(II) in a dual electrolyte, two-compartment cell separated by a bipolar membrane and powered by a solar-driven photovoltaic. The V(II) species can then be charged into a catalytic reactor, producing hydrogen and regenerating V(III).

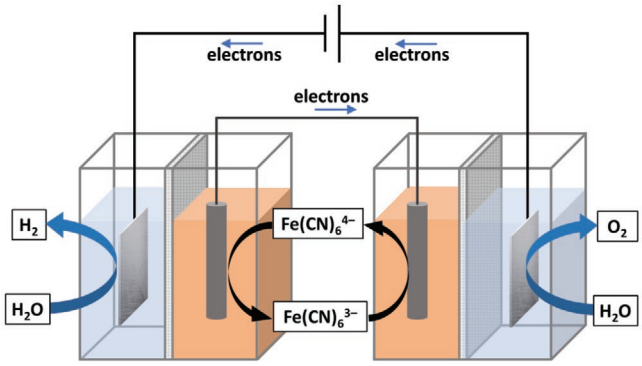

Figure 10. The closed bipolar electrode cell system used by Goodwin and Walsh to spatially decouple O_2 and H_2 production from water electrolysis.[55]

A Nafion membrane separated the two compartments in each cell, thus separating the compartment containing the closed bipolar electrode from the other, which housed a Pt electrode in 0.1 M KOH. The operation of the device involved water oxidation at a platinum electrode coupled with reduction of $Fe(CN)_6^{3-}$ at the closed bipolar electrode in one cell, while in the other, oxidation of $Fe(CN)_6^{4-}$ occurred at the other end of the closed bipolar electrode with concomitant hydrogen evolution at the second Pt electrode. Since the HER and OER were performed in entirely separate cells in this arrangement, the issue of gas mixing was eliminated. However, the rates of production of these gases remained intrinsically linked, via the closed bipolar electrode. By periodically switching the direction of the current, each redox species could be regenerated, thereby allowing continuous operation.

Since the electrolytes in the two cells in this system are entirely separated, two electrolytes at vastly different pH values can be used in the two electrochemical cells (cf. the use of bipolar membranes by Ho et al.[53]). Taking advantage of this, Goodwin and Walsh used their system to demonstrate a very elegant example of decoupled fuel cell operation. Hence, one electrochemical cell was saturated with O_2 at pH = 0 (under which conditions the oxygen reduction reaction has a redox potential of +1.23 V), whilst the other cell was saturated with H_2 at pH = 14 (under which conditions the hydrogen oxidation reaction has a redox potential of –0.83 V). Hence the total theoretical voltage output of such a fuel cell is in excess of 2 V, whereas a conventional fuel cell maintains the same pH for both chambers and therefore is limited to a total theoretical voltage output of only 1.23 V. In practice, Goodwin and Walsh were able to obtain voltage outputs >1.8 V, thus significantly exceeding the theoretical maximum performance of a conventional fuel cell under analogous conditions.

The foregoing examples almost all use somewhat extreme pH conditions (highly acidic and/or highly alkaline), in part because these are the conditions under which conventional water electrolysis has been studied in most detail. However, electrolysis under less extreme pH conditions may have benefits for materials compatibility and durability. Motivated by a desire to develop decoupling strategies that would be effective at more neutral pH values, Li et al. studied the ability of ferrocene derivatives to decouple the OER from the HER.[56] In their experimental design, (ferrocenylmethyl)trimethylammonium chloride (FcNCl) acted as the decoupling agent, undergoing oxidation and reduction in tandem with the half-reactions of water splitting. This decoupled process was performed using a two-compartment H-cell, where in one compartment, a carbon counter electrode was immersed in a 50×10^{-3} M solution of FcNCl in 0.5 M Na_2SO_4 (pH = 6.5). In the other chamber, two other electrodes were placed: Ni_2P on Ni foam to perform the HER and a Ni foam electrode to perform the OER. These electrodes were connected electrically to the electrode in the decoupling agent solution in turn, to allow temporally separated HER and OER to proceed (**Figure 11**).

FcNCl was well-suited its role as a decoupling agent on account of its high solubility in water, the position of its redox couple between the onset potentials of the OER and HER, and its stability under successive redox cycling events. When used as a decoupling agent for electrolytic water splitting, FcNCl

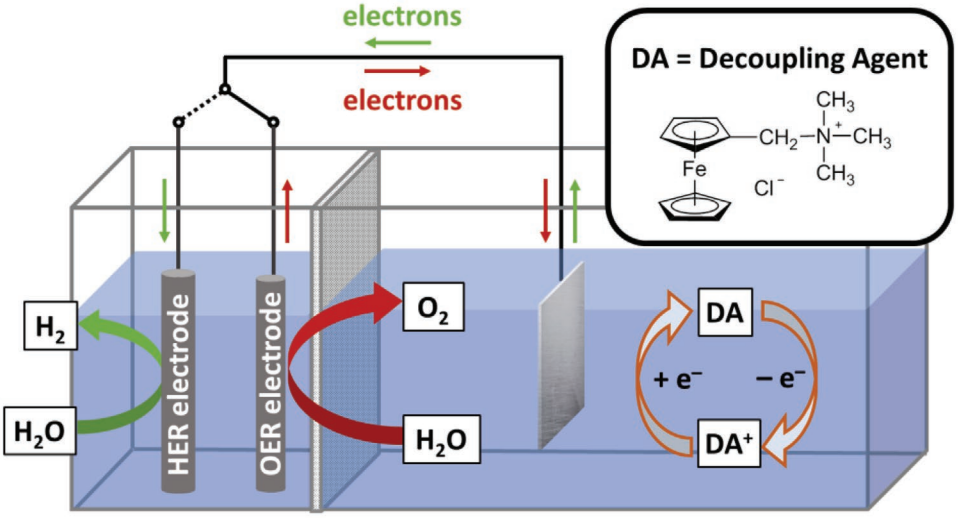

Figure 11. Experimental setup used by Li et al. with a (ferrocenylmethyl)trimethylammonium chloride decoupling agent ("DA").[56] The OER and HER were performed in consecutive steps, coupled with the reduction and reoxidation (respectively) of the decoupling agent.

was able to mediate (in turn) the OER (without simultaneous hydrogen evolution) and the HER (without simultaneous oxygen evolution) both at full Faradaic efficiency. The system proved robust to multiple successive redox cycles, despite the fact that it did not prevent the pH from varying during these cycles (the pH value of the electrolyte rose to pH 9 during the HER as protons were consumed, before decreasing back to pH 6.5 by the end of the OER process as these protons were replaced). Indeed, after 20 cycles, no change was found in the redox chemistry of the mediator, indicating its high stability to redox cycling within this pH range. Furthermore, the authors also demonstrated that sunlight-driven hydrogen production was possible with this system, by employing a photovoltaic module under solar irradiation to drive currents for the HER of around 20 mA cm^{-2} (with concomitant reoxidation of the decoupling agent). Under otherwise analogous conditions, but in the absence of decoupling agent, hydrogen production was minimal.

4. Soluble Organic Redox Mediators

Early on in the development of the concept of decoupled electrolysis, it was noted that spatial and temporal separation of oxygen evolution and hydrogen (or hydrogen-equivalent) production through the use of recyclable redox mediators had strong parallels with the mitochondrial electron transport chain. Many of the proton and electron carriers involved in such transport chains are based on quinones.[57–60] It is perhaps natural therefore to wonder whether Electron-Coupled-Proton Buffers based on quinones could be effective decoupling agents for water splitting. Such considerations motivated Rausch et al. in 2013 to investigate the simple quinone potassium hydroquinone sulfonate (derived from 1,4-hydroquinone) as a decoupling agent.[61] The addition of the sulfonate group confers water solubility on the mediator in both its oxidized and reduced forms, rendering this decoupling agent possibly the simplest water-soluble quinone-based system that could be devised. In comparison to phosphomolybdic acid that was (up to that point in time) the only other recognized example of an Electron-Coupled-Proton Buffer, potassium hydroquinone sulfonate also exhibited a significantly reduced molecular weight (≈1900 vs 228 Da) and hence the prospect of a significantly improved ratio of molecular weight to electrons stored.

Analysis of potassium hydroquinone sulfonate by cyclic voltammetry in phosphoric acid at pH 0 indicated the presence of a reversible, 2-electron redox couple at +0.65 V versus SHE; this couple therefore being suitably positioned with regard to the onset potentials of the OER and HER at this pH. Thus encouraged, decoupled electrolytic water splitting was attempted using a 0.5 M solution of the quinone derivative as the decoupling agent at a carbon electrode, and using a Pt electrode to perform the OER and then the HER in turn. Compared to a cell performing the direct electrolysis of water using this setup (OER on the Pt electrode and HER on the carbon electrode), an energy efficiency of around 80% was estimated for the decoupled system. The decoupled system was able to generate hydrogen with a Faradaic efficiency of 98%, with almost complete decoupling of this hydrogen production from oxygen production (the amount of O_2 production that was observed during the HER step in the decoupled system amounted to less than 2% of the amount of oxygen that would be expected in conventional (coupled) water electrolysis). Similarly, the decoupled system was found to produce oxygen with a Faradaic efficiency of 91 ± 5%; production of hydrogen during this step was not detected. Decoupling of the OER and HER was thus demonstrated. The pH change measured during the HER was relatively small when using this decoupling agent, suggesting that the quinone derivative was reversibly accepting both electrons and protons and acting as an effective Electron-Coupled-Proton Buffer. However, the stability of the buffer was greatly inferior to that of phosphomolybdic acid. Indeed, over 20 oxidation/reduction cycles, the charge storage capacity of this hydroquinone sulfonate Electron-Coupled-Proton Buffer was found to reduce by 1% per cycle, which was attributed to oligomerization of the oxidized form of the quinone derivative. Similarly, the quinone displayed rather a high rate of crossover through the Nafion membrane employed to stop the buffer from accessing the OER/HER compartment (≈2.7×10^{-6} mol h^{-1}). The authors proposed that both of these issues might be overcome through the use of a larger, more sterically hindered quinone derivative that would cross the membrane more slowly and be less prone to oligomerization.

To this end, some of the same authors later examined the use of anthroquinone-2,7-disulfonic acid (AQDS) as an alternative quinone-based Electron-Coupled-Proton Buffer,[62] a choice inspired in part by the successful utilization of this molecule as a stable 2-electron redox couple in an all-organic redox flow battery.[63] Cyclic voltammetry of AQDS revealed that the compound had a reversible redox couple centered around +0.21 V versus SHE, and prolonged electrochemical cycling (100 cycles of consecutive oxidation and reduction) of this couple in a two-compartment cell in 1 M H_2SO_4 revealed a decay in total capacity after these cycles of only 5.75%, representing a marked improvement over the hydroquinone sulfonate system. Analysis of the gaseous products of this redox cycling indicated that oxygen and hydrogen were produced in their respective steps with excellent decoupling, both at 100% Faradaic efficiency. These results taken together illustrated the suitability of AQDS for use as an Electron-Coupled-Proton Buffer in decoupled water splitting. The authors then assembled a dual flow cell system, consisting of two back-to-back electrolyzers. In this system, water oxidation was carried out in one cell with accompanying Electron-Coupled-Proton Buffer reduction. The reduced AQDS was then routed to the second cell, where hydrogen was produced in tandem with reoxidation of the AQDS. To reach current densities of 1 A cm^{-2}, the decoupled OER and HER steps required 2.01 and 0.96 V, respectively. Using the higher and lower heating values of hydrogen, energy efficiencies of 63% and 52% respectively were calculated for the ratio of electrochemical energy required to produce the hydrogen versus the energy that could be obtained from the combustion of that amount of hydrogen. However, after continuous operation for over 24 h at a current density of 0.25 A cm^{-2}, the potentials required to maintain this current density on the OER and HER cells rose by 33 and 103 mV, respectively, suggesting that buffer degradation remains only a partially solved problem in this system.

5. Solid State Redox Mediators

5.1. $NiOOH/Ni(OH)_2$ Electrodes

In all the examples of decoupled electrolysis listed thus far, the decoupled reactions have been mediated by species dissolved in the electrolyte. However, there is no strict requirement for the decoupling agent to be a soluble molecular species, and indeed solid-state decoupling agents bring unique capabilities to decoupled systems on account of their heterogeneous nature. The first acknowledged example of a solid-state decoupled electrolysis system was reported by the groups of Wang and Xia in early 2016,[64] using $NiOOH/Ni(OH)_2$ as the decoupling agent (a choice inspired by the charge/discharge reactions of $NiOOH/Ni(OH)_2$ when used as the cathode in commercial alkaline batteries).[65] The authors supported their nickel hydroxide on carbon nanotubes to create a solid-state mediator/electrode system, which was used to decouple the OER and HER of water splitting at high pH. The equations operating in this system are shown in Equations (9) and (10), and further illustrated in **Figure 12**. Hence, in the HER step, oxidation of $Ni(OH)_2$ to NiOOH (in which the Ni^{2+} center is oxidized to Ni^{3+}) is coupled to the production of hydrogen (Equation (9)). The decoupling agent is then rereduced to $Ni(OH)_2$ with concomitant oxygen production in the OER step.

$$Ni(OH)_2 \rightarrow NiOOH + \frac{1}{2}H_2 \tag{9}$$

$$2NiOOH + H_2O \rightarrow 2Ni(OH)_2 + \frac{1}{2}O_2 \tag{10}$$

Using cyclic voltammetry, the researchers confirmed that the $NiOOH/Ni(OH)_2$ redox couple fell between the onset potentials of the HER and OER. The system was then tested by performing 100 redox cycles, with voltage readings suggesting stable operation under these consecutive H_2 and O_2 generation steps. In situ differential electrochemical mass spectrometry was used to analyze the purity of the gaseous products formed. In the hydrogen evolution step, no O_2 above the background level was detected. Similarly, analysis of the gases produced in the oxygen evolution step revealed that no H_2 was generated, and thus that the $NiOOH/Ni(OH)_2$ electrode had completely decoupled the two half-reactions of water splitting. The gaseous products were quantified, and Faradaic efficiencies for both the HER and OER were >90%. The authors then demonstrated how the reduction of the NiOOH electrode used in the oxygen evolution step (Equation (10)) could be coupled with the oxidation of Zn(0) to Zn^{2+} (rather than the oxidation of water/hydroxide), forming a NiOOH-Zn battery. When tested at a current of 200 mA, this battery was found to have a discharge voltage of ≈1.6 V with a total discharge time of ≈10 min. NiOOH could then be regenerated by carrying out the hydrogen evolution step (Equation (9)), essentially recharging the battery. Hence this study again highlights the opportunities for new approaches to flexible energy storage and conversion that are afforded by the use of electrochemical decoupling strategies.

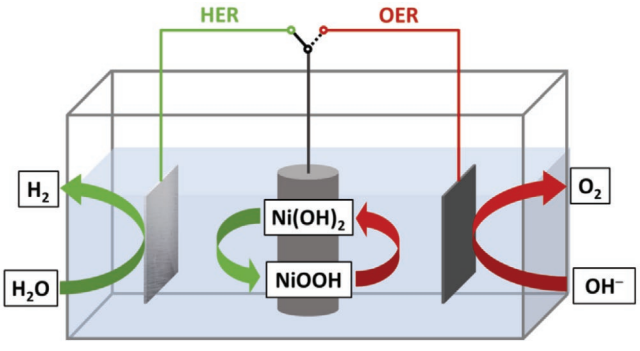

Figure 12. Schematic illustrating the mode of action of $NiOOH/Ni(OH)_2$ as a solid decoupling agent electrode. OER is coupled to NiOOH reduction (red arrows) and HER is coupled to $Ni(OH)_2$ oxidation (green arrows).

Independently to Wang and Xia, the groups of Grader and Rothschild reported the use of the same $NiOOH/Ni(OH)_2$ mediator in a closed bipolar electrode-type system for decoupled water electrolysis under alkaline conditions.[66] Accordingly, simultaneous hydrogen and oxygen generation was achieved in two spatially separated, two-compartment cells from 1 M NaOH electrolytes. Both of the cells employed a $NiOOH/Ni(OH)_2$ electrode, linked by copper wire, and a Ni foil electrode at which the gaseous products were generated. Over the course of 20 h, at an applied current density of 5 mA cm^{-2}, the system was able to generate both H_2 and O_2 continuously. Once the cell voltage reached a certain threshold (indicating that the nickel hydroxide electrodes had been fully charged/discharged), the current polarity was reversed, driving the reactions performed in each cell in the opposite direction. Over the 20 h, the total charge/discharge time for each cycle was found to decrease in duration by an average of 0.3% per cycle; this was attributed to incomplete charging of the $NiOOH/Ni(OH)_2$ electrode in the HER cell. Following this, the researchers performed longer cycles (>6 h) where the electrodes were charged to 448 mAh (≈34% of their rated capacity), with the overall experiment lasting 125 h. Analysis of the product gases revealed that H_2 and O_2 were produced at ≈100% Faradaic efficiency. The $NiOOH/Ni(OH)_2$ closed bipolar electrode cell arrangement was also integrated with an Si photovoltaic module to form a solar-powered water splitting system, and a solar-to-hydrogen conversion efficiency of 7.5% was achieved. This result was comparable to those obtained with the state-of-the-art solar-powered water splitting systems at time of writing.[67–71]

Some of the same authors subsequently demonstrated that the oxygen evolution/mediator reduction step of $NiOOH/Ni(OH)_2$ could be rendered spontaneous, thus removing one set of electrochemical losses from the system.[72,73] Using a cobalt-doped nickel hydroxide electrode ($Ni_{0.9}Co_{0.1}(OH)_2$), the hydrogen evolution step was first performed electrochemically at 25 °C (in an analogous fashion to Equation (9)), to generate the oxidized form of the cobalt-doped nickel hydroxide electrode ($Ni_{0.9}Co_{0.1}OOH$). This "charged" electrode was then removed from the electrolysis cell and placed in 5 M KOH which had been heated to 95 °C, at which temperature the decomposition reaction of $Ni_{0.9}Co_{0.1}OOH$ to regenerate $Ni_{0.9}Co_{0.1}(OH)_2$ (releasing O_2 in the process) is both exothermic and spontaneous. This system was tested using consecutive 100-second cycles of hydrogen and oxygen production, at a fixed current

density of 50 mA cm^{-2}, evincing a voltage efficiency of 98.7% (voltage efficiency = V_{th}/V_{cell}, where V_{th} is the thermoneutral voltage of water splitting). As the oxygen evolution step in this system was spontaneous at 95 °C and as the energy for this thermal step could be provided by waste heat, the overall efficiency of this process has the potential to be considerably higher than for systems where both oxidation and reduction of the $NiOOH/Ni(OH)_2$ couple are performed electrochemically.

Recently, the Grader and Rothschild groups have demonstrated decoupled hydrogen and oxygen production using $NiOOH/Ni(OH)_2$ electrodes driven purely by solar irradiation, whereby the O_2 and H_2 are produced in entirely different cells which are connected only electrically.[74] A schematic of the concept behind this setup is shown in **Figure 13**, which used a closed-bipolar-type $NiOOH/Ni(OH)_2$ electrode. The oxygen-evolving cell contained a hematite (α-Fe_2O_3) photoanode, which was interfaced with a monocrystalline silicon photovoltaic module to provide additional potential bias. Indeed, this photoanode/photovoltaic ensemble provided sufficient energy to drive all of the electrochemical reactions that ensued. O_2 was evolved in this cell with simultaneous reduction of the NiOOH electrode also present in the cell. Meanwhile, in the separate hydrogen evolution cell, the H_2 was evolved at a Pt-coated Ti mesh cathode as $Ni(OH)_2$ was oxidized. Compared to solar-driven decoupled electrolysis protocols that use soluble redox mediators, this approach has the advantage that there is no need to pump any decoupling agent solutions between cells, and therefore no need for membrane separators. However, the main disadvantage is that the solid-state decoupling agent electrodes have a finite capacity, and that they must be replaced (or swapped round) once they reach this capacity limit in order for electrolysis to continue. Using a system whereby multiple $NiOOH/Ni(OH)_2$ electrodes were present in each cell and used in succession, the authors were able to carry out ten water splitting cycles of over eight hours' duration each, producing hydrogen and oxygen at an average current of 55 mA and a solar-to-hydrogen efficiency of ≈0.7%.

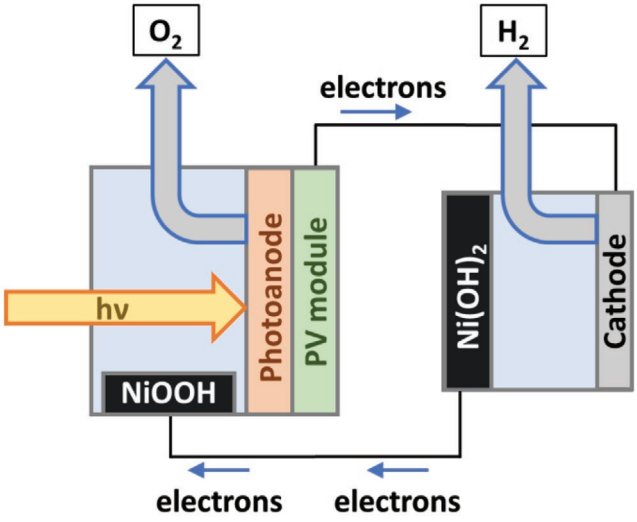

Figure 13. The system employed by Landman et al.[74] whereby oxygen is produced in a photoelectrochemical-photovoltaic tandem cell and hydrogen is produced separately in a conventional electrochemical cell, using separated NiOOH and $Ni(OH)_2$ electrodes to decouple the OER and HER.

5.2. Other Solid Metal Oxides

Soon after the publication of $NiOOH/Ni(OH)_2$ as a decoupling agent, Xiao and co-workers reported the use of FeO_x as a solid state mediator electrode.[75] Their system employed three electrodes: an Ni-Fe anode, a Pt/C cathode, and the FeO_x solid state mediator electrode (supported on Ni foam). During charging, oxygen was evolved at the Ni-Fe anode as the FeO_x (in the same compartment of the electrochemical cell) underwent a two-electron reduction. Then, during discharge, hydrogen was produced at the Pt/C cathode (in a separate compartment, separated from the first compartment by an anion exchange membrane) alongside reoxidation of FeO_x decoupling agent. The performance of the device was assessed by carrying out 50 consecutive charge/discharge cycles, showing that the capacity retention and Faradaic efficiency were 97% and >90%, respectively. The authors were also able to demonstrate solar-powered decoupled electrolysis, by substituting the Ni-Fe anode for a TiO_2/Co-Pi photoanode and exposing this to sunlight. The solar-to-hydrogen conversion efficiency of this configuration was found to be 3.3%.

In 2017, Choi et al. employed a manganese dioxide mediator electrode to decouple the half-reactions of water splitting.[76] This mediator electrode was used in a three-electrode setup alongside an $Ni(OH)_2$ positive electrode and a lanthanum-nickel metal hydride negative electrode. Both hydrogen and oxygen were produced in separate steps as a function of which electrodes were connected; in the first step, the oxygen evolution reaction was accompanied by the reduction of the mediator electrode (Equation (11)), whilst in the second step the oxidation of MnOOH (Equation (12)) occurred with simultaneous reduction of water to form hydrogen.

$$2MnO_2 + H_2O \rightarrow 2MnOOH + \frac{1}{2}O_2 \quad (11)$$

$$2MnOOH \rightarrow 2MnO_2 + H_2 \quad (12)$$

In this cell, a current of 5 mA was maintained over 10 h for both steps, at 25, 40, and 60 °C. Although the oxygen and hydrogen generation steps could be effectively decoupled, the authors noted that the energy conversion efficiency of their system was low in comparison to conventional (i.e., coupled) devices, which they attributed to the high overpotentials associated with the use of the MnO_2 electrodes.

5.3. Solar-Thermal Decoupled Electrolysis

When heated to high temperatures in air, certain transition metal oxides can be reduced to lower oxides with the release of oxygen. For example, at temperatures above 1370 °C, the process

$$3Fe_2O_3 \rightarrow 2Fe_3O_4 + \frac{1}{2}O_2 \quad (13)$$

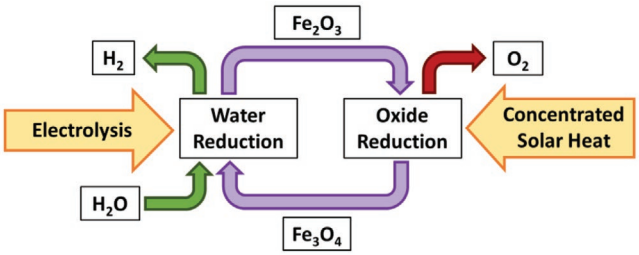

Figure 14. The solar thermal decoupled process proposed by Palumbo et al.[77] using the example of iron oxides.

occurs, and similar thermal decomposition reactions are known for Co and Mn oxides. Palumbo et al. used this as their starting point for assessing the prospects for a combined thermal-electrochemical cycle for decoupled water splitting, for these three metal oxides, according to the general scheme shown in **Figure 14**.[77]

According to this scheme, thermally generated magnetite (Fe_3O_4) can be reoxidized electrochemically to give Fe_2O_3, with simultaneous hydrogen generation occurring at the cathode. The oxygen and hydrogen generation steps are thus completely decoupled via the use of this metal oxide mediator. Palumbo et al. demonstrated the feasibility of the electrochemical aspects of this work using a cell design such as that shown in **Figure 15**. Fe_3O_4 was suspended in either H_2SO_4 or KOH, forming a slurry of magnetite particles in the electrolyte. Due to gravity, the magnetite particles tend to sink toward the bottom of the cell, leaving the upper part of the cell free of particles (and hence just electrolyte solution to a first approximation). Through judicious choice of stirring rates, the authors were able to maintain two regions (one with particles, and one without) in their cell throughout the electrolysis. Into the slurry region of the cell was placed a Pt foil electrode to act as the anode. Meanwhile, a Pt-coated Mo wire was inserted into the top half of the cell to act as the cathode. Electrolysis was then initiated in order to oxidize the magnetite particles, whilst simultaneously generating hydrogen at the cathode. Gas chromatography analysis of the headspace of the cell revealed that hydrogen was produced in this experiment with a Faradaic efficiency of ≈100%. Moreover, no oxygen was detected during electrochemical hydrogen generation, suggesting complete decoupling of the HER from oxygen production. Instead, a yellow powder was observed to form in the slurry as the primary product of electrochemical oxidation; unreacted magnetite was separated from this product through the use of magnets. Powder X-ray diffraction then revealed that the yellow product was FeOOH. The authors then completed the thermal-electrochemical cycle by heating this FeOOH to 1400 °C at a rate of 10 °C min^{-1}, whereupon simultaneous thermogravimetric and differential scanning calorimetry analyses indicated that the FeOOH was first thermally dehydrated to Fe_2O_3, before this Fe_2O_3 underwent thermal reduction to produce Fe_3O_4 with release of O_2 (Equation (13)). Some of the same authors subsequently showed that a similar thermal-electrochemical cycle for decoupled oxygen and hydrogen production from water was also possible with cobalt oxides.[78] This approach is somewhat remarkable in that the decoupling agent is neither a monolithic electrode, nor a soluble molecular species. Instead, the decoupling agent is a suspension of otherwise insoluble particles. Whether or not such a system could be implemented on a large scale for continuous operation remains to be seen, but the concept certainly seems to merit further study.

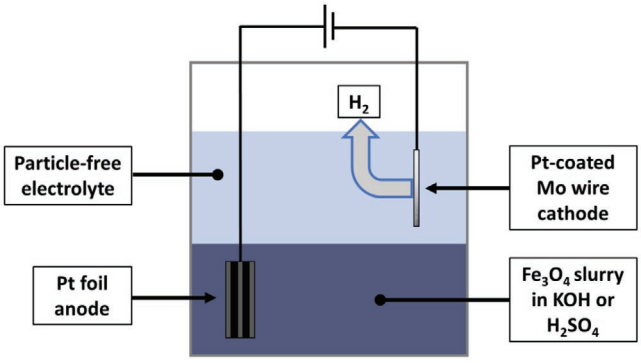

Figure 15. The layered electrochemical cell employed by Palumbo et al.[77] using the example of iron oxides.

5.4. Solid Organic Decoupling Agents

Decoupling of the HER and OER has also been described using reversible n-type doping of the solid-state battery material, polytriphenylamine (PTPAn).[79] The organic polymer PTPAn has a structure consisting of conductive polyparaphenylene chains on which electroactive polyaniline units are attached (see **Figure 16**a), giving the material excellent reported redox cycling stability, and making it well-suited for use as a redox mediator.[80–82] In acidic electrolyte (0.5 M H_2SO_4), cyclic voltammetry performed by Wang and co-workers indicated that PTPAn has two redox couples which reside between the onset voltages of the HER and OER. For the decoupled water electrolysis experiments, hydrogen was evolved at a Pt-coated Ti mesh electrode while RuO_2/IrO_2-coated Ti mesh was used as the oxygen evolving electrode; these reactions followed Equations (1) and (2), respectively. Galvanostatic electrolysis at a current of 100 mA was found to produce hydrogen and oxygen with Faradaic efficiencies approaching 100%. Decoupled electrolysis was then driven using an Si photovoltaic module to demonstrate that the system could convert solar energy and water directly to H_2 and O_2. A solar-to-hydrogen conversion efficiency of 5.4% was achieved using this photovoltaic system, when exposed to sunlight.

In 2019, some of the same authors reported the use of pyrene-4,5,9,10-tetraone (PTO) as a solid-state mediator to successfully decouple hydrogen and oxygen production from water.[83] In this study, the HER and OER were separately coupled to the reversible enolization reaction of PTO (Figure 16b). In contrast to PTPAn, this PTO-based mediator undergoes reversible protonation and deprotonation during redox cycling and so has the potential to buffer the solution pH during operation. Cyclic voltammograms taken of the compound revealed two reversible redox couples which both fell between the onset potentials of the HER and OER when using a Pt-coated Ti mesh cathode and RuO_2/IrO_2-coated Ti mesh anode. This analysis also revealed that the redox processes of PTO were not

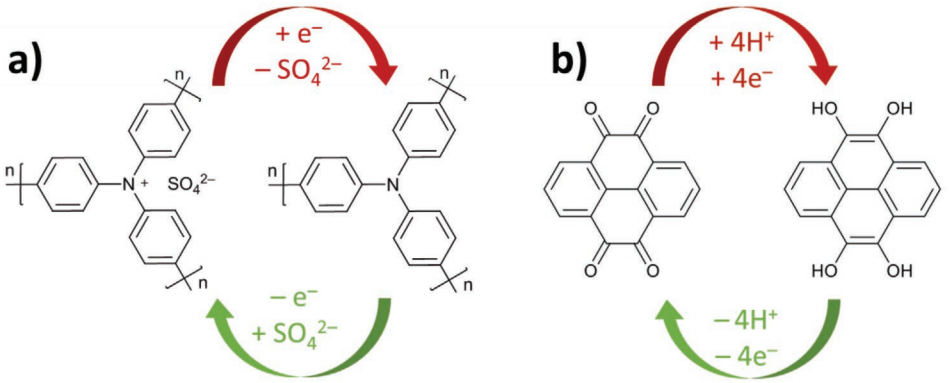

Figure 16. a) The polytriphenylamine (PTPAn) redox couple employed by Wang and co-workers.[79] b) The pyrene-4,5,9,10-tetraone (PTO) redox couple.

diffusion limited, suggesting that the buffer is indeed in the solid state. The mediator performed well for decoupled oxygen and hydrogen evolution during electrolytic water splitting in 0.5 M H_2SO_4 over multiple cycles, with Faradaic efficiencies for both gases approaching 100%.

Finally in this section, the conducting polymer polyaniline has also been utilized as an electrode material to decouple the HER and OER under acidic conditions.[84] Wang et al. carried out cyclic voltammetry on polyaniline film electrodes, after pressing a powder of the polymer onto Ti mesh. They discovered two redox couples, which they attributed to two different doping states of polyaniline; both of these couples had redox potentials between the onset potentials of the HER and OER. Decoupling experiments were performed in 0.5 M H_2SO_4, in a three-electrode configuration, with a Pt HER electrode and a RuO_2/IrO_2 electrode for the OER. When assessing the charge storage capabilities of polyaniline, the authors found that it far exceeded several other redox mediators, such as phosphomolybdic acid and PTPAn. Using a charge–discharge rate of 0.2 A g^{-1}, the reversible discharge capacity of polyaniline was found to be 125 mAh g^{-1}. At this same charge–discharge rate, the stability of polyaniline under consecutive cycling was also investigated. It was found that over 40 cycles, the Coulombic efficiency of the cycling remained at ≈100%; capacity retention after this cycling was also high (92%). To investigate the suitability of this system for solar applications, the researchers employed an Si solar cell as a power source. With an applied potential of ≈1.0 V from the solar component, decoupled water splitting was achieved when using the polyaniline mediator electrode, although no solar-to-hydrogen conversion efficiency is quoted.

6. Decoupled Electrolysis for Chemical Synthesis

The ability to store electrons for extended periods of time on reduced decoupling agents raises the prospect of using these species as reducing equivalents for chemical processes other than hydrogen generation. This approach has two especially attractive features. First, if these reduced decoupling agents are produced using electrons (and protons) derived from water, then they constitute sustainable reducing equivalents. Second, those decoupling agents that also store protons (Electron-Coupled-Proton Buffers) can in theory be used as hydrogenation agents, replacing gaseous hydrogen as a reagent. Ultimately, this could lead to the replacement of dangerous and/or toxic chemical reagents by sustainable electricity and water.

The polyoxometalate silicotungstic acid has found utility in this regard as a sustainable hydrogenation agent for a number of organic transformations. In 2018, MacDonald et al.[87] used the two-electron reduced form of this compound ($H_6SiW_{12}O_{40}$, which they generated electrochemically with concomitant oxidation of water) as a source of protons and electrons for the reduction of a range of nitroarene compounds to their aniline analogues in (on the whole) good to excellent yields (**Figure 17**a). The silicotungstic acid could then be recycled, rereduced, and reused without any appreciable drop in catalytic performance. Intriguingly in this example, it was found that $H_6SiW_{12}O_{40}$ was effective for these hydrogenation reactions without the need for any cocatalyst, thus providing distinct advantages over traditional chemical approaches to nitroarene reduction (e.g., the use of H_2 gas with a Pt/C catalyst or the use of sacrificial soluble hydrogenation agents with various cocatalysts).

Wu et al. have used the same compound ($H_6SiW_{12}O_{40}$, also prepared through decoupled electrolysis with simultaneous water oxidation) to perform the hydrogenation of phenylacetylene and acetophenone (Figure 17b).[85] In this case, a Pt/C or Pd/C catalyst was found to be essential for reductive activity. Ethanol/water mixtures were used as the media for both the hydrogenation reactions (to improve substrate solubility) and for the electrochemical generation of $H_6SiW_{12}O_{40}$. The maximal conversions of phenylacetylene and acetophenone were 100% and 80% respectively, and some selectivity over the products' depth of reduction could be obtained by alteration of the reaction conditions. Taken together, these two studies suggest that reduced soluble decoupling agents have considerable potential as sustainable and easy-to-handle hydrogenation agents for organic synthesis.

Decoupled electrolysis has also been employed in reactions where organic substrates are oxidized. Li et al. used the decoupling agent $Na_4[Fe(CN)_6]$ (which they also showed to be effective for decoupled water electrolysis) to decouple the HER from the oxidation of 5-hydroxymethylfurfural to 2,5-furandicarboxylic acid.[56] 5-Hydroxymethylfurfural is a readily available product of dehydration of certain sugars and thus constitutes a sustainable feedstock chemical; the authors proposed that

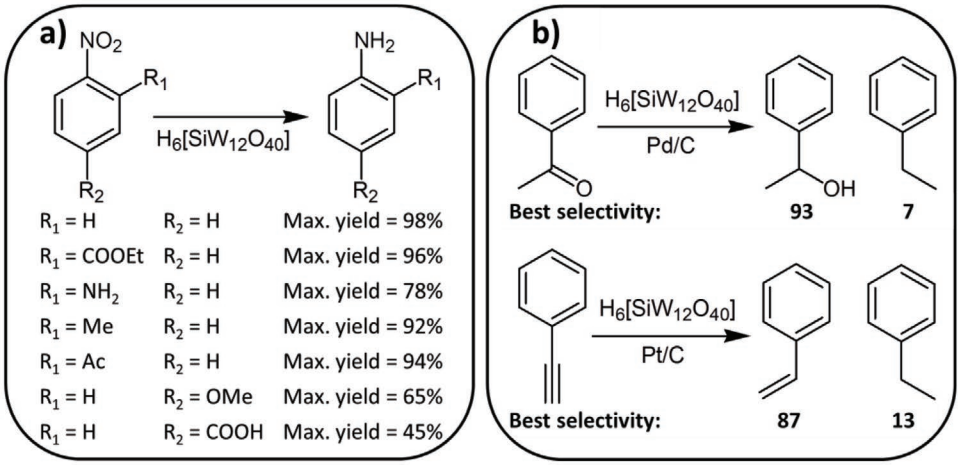

Figure 17. Organic transformations mediated by reduced silicotungstic acid prepared by decoupled water electrolysis: a) Reductions of nitroarenes as reported by MacDonald et al.[87] b) Hydrogenation of phenylacetylene and acetophenone as reported by Wu et al.[85]

its chemical transformation to 2,5-furandicarboxylic acid represented a higher-value anodic counterpart for hydrogen evolution than the oxidation of water. Accordingly, the authors assembled a two-compartment cell separated by a cation exchange membrane. The HER was first performed at a CoP on carbon electrode, with concomitant oxidation of the decoupling agent at the carbon counter electrode. In the second step, this mediator was rereduced as 5-hydroxymethylfurfural oxidation occurred at a Ni anode. 100% conversion of 5-hydroxymethylfurfural (giving an 83% yield of 2,5-furandicarboxylic acid) was reported, using mild electrochemical conditions. This approach could offer an effective and environmentally friendly approach for combining the electrolytic production of hydrogen with the generation of useful chemicals in situations where sustainably sourced organic feedstocks are available.

This $Fe(CN)_6^{3-}/Fe(CN)_6^{4-}$ decoupling agent has also been employed by You and co-workers to decouple hydrogen production from the oxidation of organic pollutants during electrochemical decontamination of wastewater.[86] In a conventional electrochemical cell for oxidation of organic pollutants, the corresponding cathode reaction is the generation of hydrogen. The authors suggested that this presents a hazard under some conditions and is also wasteful, as the H_2 is rarely harvested. They therefore proposed decoupling as a route by which hydrogen generation could take place outside the pollutant oxidation cell, for safety and ease of hydrogen collection. In a system similar to that used by Goodwin and Walsh,[55] two separate two-compartment cells were bridged by a closed bipolar electrode. This allowed the generation of hydrogen via water splitting at a Pt/C cathode, with concomitant oxidation of $Fe(CN)_6^{4-}$ to $Fe(CN)_6^{3-}$ at the anode, to occur in one cell. In the other cell, oxidation of the organic pollutant phenol was achieved on a TiSO anode, with accompanying $Fe(CN)_6^{3-}$ reduction to $Fe(CN)_6^{4-}$ at the cathode. At current densities of 16 mA cm^{-2}, the phenol removal efficiency at the TiSO anode over 2 h was found to exceed 96%, whilst the Faradaic yield for hydrogen production at the Pt/C cathode in the other cell was quantitative. This hydrogen was generated in a separate cell to the organic oxidation reaction (which generates O_2 as a side product) and so required no further purification. The authors argued that this separation of the product gases would decrease the complexity of any scaled-up version of the process as well as allowing a portion of the energy spent on the anodic oxidation of pollutants (10–20%) to be recovered in the form of hydrogen fuel.

The final examples of the application of decoupled electrolysis for performing reactions beyond water splitting that we shall consider both relate to the chlor-alkali process. In the chlor-alkali process, a sodium chloride solution is electrolyzed to generate Cl_2, H_2, and NaOH as the products. Together, these products are themselves used in over 50% of all industrial processes, underlining the fundamental importance of the chlor-alkali process to the chemical industry at large. Historically, Cl_2, H_2, and NaOH were produced in mercury-containing cells according to the Castner–Kellner process (itself an electrochemical decoupling strategy, whereby Cl_2 and H_2 evolution are decoupled using a mercury amalgam electrode as the decoupling agent).[88] In recent years, however, mercury cells have fallen out of favor due to concerns over mercury's toxicity. Hence, most chlor-alkali cells now use either asbestos diaphragms or fluorine-containing ion-exchange membranes to separate the chlorine and hydrogen that are produced. However, Hou et al. argued that the high cost of these separators and their short lifetimes during operation made the need for improvements vital. Therefore, these authors proposed a membrane-free process whereby the Cl_2 evolution and H_2/NaOH production steps were decoupled by employing the reversible Na-ion intercalation/deintercalation reaction of an $Na_{0.44}MnO_2$-based electrode.[89]

An illustration of this decoupled process and the reactions involved is provided in **Figure 18**. Hence water reduction to generate H_2 and hydroxide is accompanied by sodium deintercalation from the decoupling agent electrode. Subsequently, chloride ions are oxidized to Cl_2 with the simultaneous reduction of the decoupling electrode, which occurs together with reintercalation of sodium ions to restore the original $Na_{0.44}MnO_2$ stoichiometry. The $Na_{0.44}MnO_2$-based electrode has previously been employed in sodium ion batteries and so displays the required sodium ion intercalation/deintercalation properties; its redox

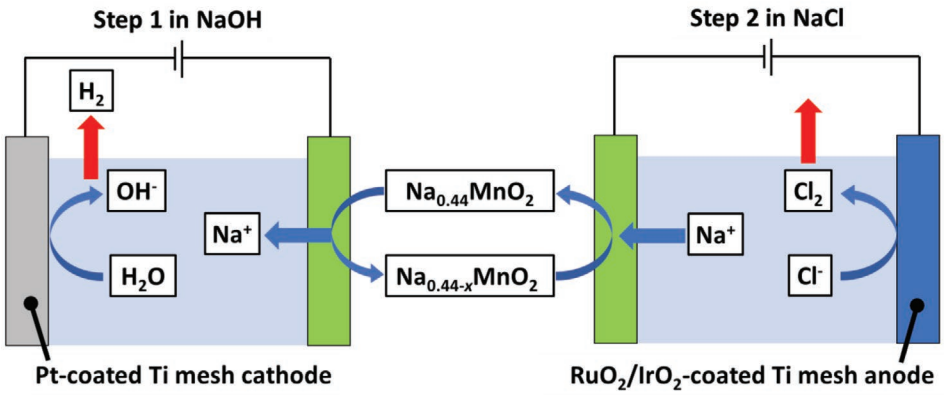

Figure 18. The two-step decoupled chlor-alkali process reported by Hou et al.[89]

waves are also almost exactly midway between the onset potentials of hydrogen and chlorine evolution.

In the first step, hydrogen evolution on a Pt-coated Ti-mesh electrode was found to proceed at a Faradaic efficiency of 100%, whilst in the second step, chlorine evolution on a RuO_2/IrO_2-coated Ti mesh displayed a Faradaic efficiency of 90%, which the authors attributed to the hydrolysis of Cl_2 to give soluble species such as HClO. The authors also noted that the current density that the system can reach is limited by the kinetics of sodium ion intercalation/deintercalation into and out of the $Na_{0.44}MnO_2$-based electrode. Technologically relevant current densities for the HER and chlorine evolution reactions of up to 0.5 A cm^{-2} were achieved, but only if very large $Na_{0.44}MnO_2$ electrodes were employed. Attempting to improve the kinetics of this intercalation/deintercalation process would therefore be one area in which further investigation could prove beneficial, and which might bring about the realization of some of the benefits of decoupling for this reaction (including avoiding the need for a membrane separator and preventing mixing of the H_2 and Cl_2 product gases).

Zhao et al. have taken this work a step further, by proposing a system for decoupling Cl_2 and NaOH production that uses two decoupling agents and three different electrochemical cell configurations.[90] An illustration of this concept is provided in **Figure 19**.

Hence, in the first cell, oxygen reduction (to hydroxide) is paired with oxidation (and desodiation) of a $Na_{0.44}MnO_2$-based electrode to generate NaOH. The desodiated $Na_{0.44-x}MnO_2$ electrode is then placed in a chloride-containing electrolyte and used as the cathode in a second electrolysis cell, alongside a silver anode. Operating this cell rereduces (and resodiates) the $Na_{0.44}MnO_2$ electrode, whilst at the anode insoluble AgCl forms. In the final step, the AgCl electrode is used as the cathode in a third electrolytic cell alongside a graphite anode. As the AgCl is reduced (regenerating Ag(0)), chloride ions are released which migrate to the anode where they are discharged as Cl_2. The overall reaction thus produces no hydrogen and is

$$4Na^+ + 4Cl^- + O_2 + 2H_2O \rightarrow 4NaOH + 2Cl_2 \quad (14)$$

The authors suggested that such an approach decouples NaOH and chlorine production and so prevents the production of caustic chlorates which could otherwise damage the $Na_{0.44}MnO_2$ electrode. Using oxygen as the reductive couple in the first cell was also held to reduce the overall voltage requirement for Cl_2 and NaOH production. Excellent stability to multiple redox cycles was demonstrated for each of the three processes, with high Coulombic efficiencies. Moreover, the authors were also able to show that this concept can be expanded to other salts, e.g., to the continuous production of NaOH and

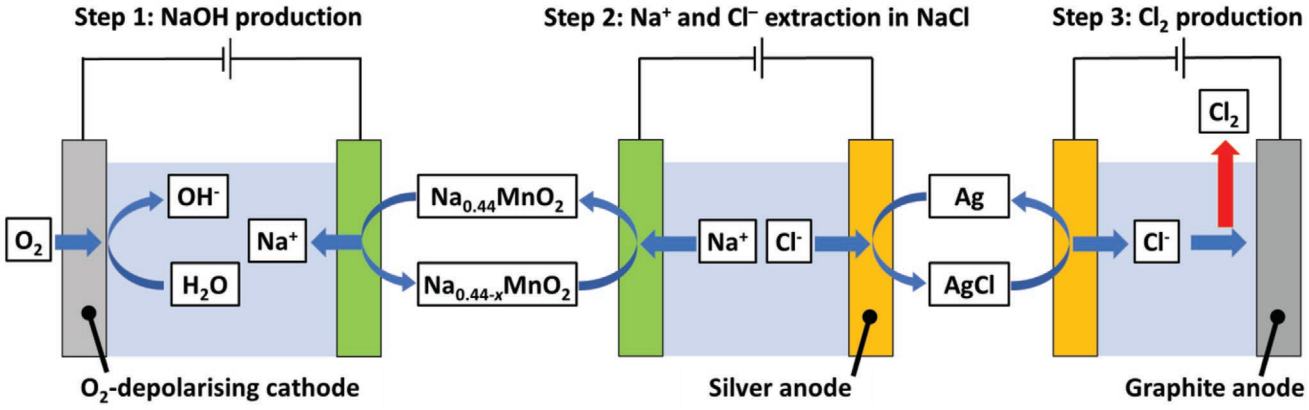

Figure 19. The three-step decoupled chlor-alkali process reported by Zhao et al.[90]

HNO_3 from a solution of $NaNO_3$. This route therefore offers considerable promise, although it may prove nontrivial to design large-scale systems where multiple electrodes are easily switched between cells.

7. Conclusions and Outlook

In this review, we have examined the current state-of-the-art in decoupled electrolysis for water splitting, following the development of the field from its conceptualization in 2013 through to the numerous elaborations of decoupled electrolysis that have since been developed. Key milestones along this journey have included the demonstration of solar-driven hydrogen production using decoupling strategies, the discovery of decoupling agents that can be induced to perform one of the half-reactions of water splitting spontaneously (e.g., by manipulation of the temperature or by suitable choice of electrodes and/or catalysts), the development of robust solid-state decoupling agents, the conjunction of decoupling strategies with bipolar electrolysis, and the application of decoupling strategies to reactions beyond water splitting (e.g., coupling H_2 production with organic upgrading oxidation reactions or performing organic hydrogenation reactions using protons and electrons derived from water). Furthermore, it will be apparent that decoupling can be applied both for electrolytic processes (i.e., those requiring a net energy input such as water splitting) and galvanic processes (where spontaneous chemical reactions are harnessed to produce electrical power as in fuel cells).

A number of key challenges remain in the development of decoupled electrolysis. The majority of these can be distilled into just two main brackets: device complexity and overall system stability. In terms of the latter, materials compatibility between the decoupling agents and other cell components (e.g., membrane separators) and the stability of the agents themselves to repeated redox cycling often remains unproven, largely due to a lack of data on the long-term performance of decoupled systems (as indicated, for example, by the "Number of Cycles Tested" column in Table 1). Robust data on long-term system stability must be obtained before commercial applications become a reality. Meanwhile, decoupled electrolysis systems often give rise to increased requirements for additional balance of plant (and hence involve greater complexity) compared to simpler, coupled approaches. For decoupling agents in solution, this manifests as a requirement for additional pumps and flow systems, and often the decoupling agent solutions are more viscous than water or other commonly encountered solvents. For solid-state decoupling agents, developing workable protocols for continuous operation of the resulting systems will be crucial for the wider adoption of this approach, especially if such continuous operation relies on the physical relocation of the decoupling agent, or the use of complicated manifold flowpaths for electrolytes. Such challenges are probably not insurmountable, but nevertheless they constitute considerable barriers that decoupled electrolysis systems will have to overcome in order to fulfil their promise.

The ability to keep the products of electrolysis separate is one of the key advantages of decoupled electrochemistry and it is probably in this area that most future work will concentrate in the near term due to the obvious benefits this has for solar-to-hydrogen devices. Likewise, solar-driven electrochemical processes of all sorts can benefit from the decoupling of the rates of the relevant half-reactions that this process allows: slow, solar intensity-limited processes can be used to trickle-charge decoupling agents, which can then be used in more rapid reactions that are not limited by the instantaneous solar flux. Again, the benefits for the collection of hydrogen from solar-driven water splitting are obvious and have been highlighted by a number of the studies discussed in this review. In the longer term, we anticipate that the ability to use electrochemical decoupling as a means to obtain sustainable reduction equivalents (e.g., hydrogen equivalents from water) will have considerable impact on chemical synthesis in general. Approaches of this nature may include further elaboration on the organic hydrogenation reactions that are discussed above, but perhaps more excitingly could also include new concepts and device designs for critical underpinning processes such as CO_2 and N_2 reduction. Given the rapid progress and immense creativity that has already been in evidence in the field, it seems that the future of decoupled electrolysis is bright.

Acknowledgements

M.D.S. thanks the Royal Society for a University Research Fellowship (UF150104) and acknowledges the Engineering and Physical Sciences Research Council for supporting his work in this area (EP/K023004/1 and EP/R020914/1). P.J.M. and A.D.S. both thank the Royal Society for Ph.D. scholarships. The authors note that a similar review has recently been published on the pre-print arXiv website.[91] This review and their own were developed in parallel by different groups of authors at different institutions and are thus completely independent of each other.

Conflict of Interest

M.S. holds two patents on the use of decoupling agents for water splitting.

Keywords

decoupled electrolysis, electron-coupled-proton buffers, hydrogen evolution reaction, oxygen evolution reaction, redox mediators, solar-to-hydrogen, water splitting

Received: July 30, 2020
Revised: September 29, 2020
Published online: October 13, 2020

[1] P. D. Noyes, M. K. McElwee, H. D. Miller, B. W. Clark, L. A. Van Tiem, K. C. Walcott, K. N. Erwin, E. D. Levin, *Environ. Int.* **2009**, *35*, 971.
[2] L. Cheng, K. E. Trenberth, J. Fasullo, T. Boyer, J. Abraham, J. Zhu, *Sci. Adv.* **2017**, *3*, e1601545.
[3] A. Shepherd, E. Ivins, E. Rignot, *Nature* **2018**, *558*, 219.
[4] S. C. Doney, V. J. Fabry, R. A. Feely, J. A. Kleypas, *Ann. Rev. Mar. Sci.* **2009**, *1*, 169.
[5] M. Lindner, M. Maroschek, S. Netherer, A. Kremer, A. Barbati, J. Garcia-Gonzalo, R. Seidl, S. Delzon, P. Corona, M. Kolström, M. J. Lexer, M. Marchetti, *For. Ecol. Manage.* **2010**, *259*, 698.

[6] I. Roger, M. A. Shipman, M. D. Symes, *Nat. Rev. Chem.* **2017**, *1*, 0003.
[7] S. Styring, *Faraday Discuss.* **2012**, *155*, 357.
[8] N. S. Lewis, D. G. Nocera, *Proc. Natl. Acad. Sci. USA* **2006**, *103*, 15729.
[9] J. S. Wallace, C. A. Ward, *Int. J. Hydrogen Energy* **1983**, *8*, 255.
[10] S. A. Sherif, F. Barbir, T. N. Veziroglu, *Sol. Energy* **2005**, *78*, 647.
[11] C. Xiang, K. M. Papadantonakis, N. S. Lewis, **2016**, *3*, 169.
[12] S. B. Lalvani, P. Rajagopal, *J. Electrochem. Soc.* **1992**, *139*, L1.
[13] N. T. Suen, S. F. Hung, Q. Quan, N. Zhang, Y. J. Xu, H. M. Chen, *Chem. Soc. Rev.* **2017**, *46*, 337.
[14] L. M. Das, *Int. J. Hydrogen Energy* **1996**, *21*, 703.
[15] M. Carmo, D. L. Fritz, J. Mergel, D. Stolten, *Int. J. Hydrogen Energy* **2013**, *38*, 4901.
[16] G. Gahleitner, *Int. J. Hydrogen Energy* **2013**, *38*, 2039.
[17] E. M. Sommer, L. S. Martins, J. V. C. Vargas, J. E. F. C. Gardolinski, J. C. Ordonez, C. E. B. Marino, *J. Power Sources* **2012**, *213*, 16.
[18] J. Chi, H. Yu, *Chin. J. Catal.* **2018**, *39*, 390.
[19] M. Umeda, K. Sayama, T. Maruta, M. Inoue, *Ionics* **2013**, *19*, 623.
[20] J. Mališ, M. Paidar, T. Bystron, L. Brožová, A. Zhigunov, K. Bouzek, *Electrochim. Acta* **2018**, *262*, 264.
[21] I. Vincent, A. Kruger, D. Bessarabov, *Int. J. Hydrogen Energy* **2017**, *42*, 10752.
[22] J. R. Varcoe, P. Atanassov, D. R. Dekel, A. M. Herring, M. A. Hickner, P. A. Kohl, A. R. Kucernak, W. E. Mustain, K. Nijmeijer, K. Scott, T. Xu, L. Zhuang, *Energy Environ. Sci.* **2014**, *7*, 3135.
[23] C. C. L. McCrory, S. Jung, I. M. Ferrer, S. M. Chatman, J. C. Peters, T. F. Jaramillo, *J. Am. Chem. Soc.* **2015**, *137*, 4347.
[24] M. Chandesris, V. Médeau, N. Guillet, S. Chelghoum, D. Thoby, F. Fouda-Onana, *Int. J. Hydrogen Energy* **2015**, *40*, 1353.
[25] M. Schalenbach, M. Carmo, D. L. Fritz, J. Mergel, D. Stolten, *Int. J. Hydrogen Energy* **2013**, *38*, 14921.
[26] F. Barbir, *Sol. Energy* **2005**, *78*, 661.
[27] H. Janssen, J. C. Bringmann, B. Emonts, V. Schroeder, *Int. J. Hydrogen Energy* **2004**, *29*, 759.
[28] M. D. Symes, L. Cronin, *Nat. Chem.* **2013**, *5*, 403.
[29] A. G. Wallace, M. D. Symes, *Joule* **2018**, *2*, 1390.
[30] B. You, Y. Sun, *Acc. Chem. Res.* **2018**, *51*, 1571.
[31] X. Liu, J. Chi, B. Dong, Y. Sun, *ChemElectroChem* **2019**, *6*, 2157.
[32] T. E. Mallouk, *Nat. Chem.* **2013**, *5*, 362.
[33] N. Tanaka, K. Unoura, E. Itabashi, *Inorg. Chem.* **1982**, *21*, 1662.
[34] L. G. Bloor, R. Solarska, K. Bienkowski, P. J. Kulesza, J. Augustynski, M. D. Symes, L. Cronin, *J. Am. Chem. Soc.* **2016**, *138*, 6707.
[35] C. Santato, M. Ulmann, J. Augustynski, *J. Phys. Chem. B* **2001**, *105*, 936.
[36] R. Solarska, K. Bienkowski, S. Zoladek, A. Majcher, T. Stefaniuk, P. J. Kulesza, J. Augustynski, *Angew. Chem., Int. Ed.* **2014**, *53*, 14196.
[37] G. Hodes, D. Cahen, J. Manassen, *Nature* **1976**, *260*, 312.
[38] F. Li, F. Yu, J. Du, Y. Wang, Y. Zhu, X. Li, L. Sun, *Chem. Asian J.* **2017**, *12*, 2666.
[39] M. D. Bhatt, J. S. Lee, *J. Mater. Chem. A* **2015**, *3*, 10632.
[40] T. W. Kim, Y. Ping, G. A. Galli, K. S. Choi, *Nat. Commun.* **2015**, *6*, 8769.
[41] R. Singh, A. A. Shah, A. Potter, B. Clarkson, A. Creeth, C. Downs, F. C. Walsh, *J. Power Sources* **2012**, *201*, 159.
[42] T. Matsui, E. Morikawa, S. Nakada, T. Okanishi, H. Muroyama, Y. Hirao, T. Takahashi, K. Eguchi, *ACS Appl. Mater. Interfaces* **2016**, *8*, 18119.
[43] B. Rausch, M. D. Symes, G. Chisholm, L. Cronin, *Science* **2014**, *345*, 1326.
[44] G. Chisholm, L. Cronin, M. D. Symes, *Electrochim. Acta* **2020**, *331*, 135255.
[45] *Installation Permitting Guidance for Hydrogen and Fuel Cell Stationary Applications: UK Version*, Health and Safety Laboratory, Derbyshire, UK, http://www.hse.gov.uk/research/rrpdf/rr715.pdf (accessed: July 2020).
[46] L. MacDonald, J. C. McGlynn, N. Irvine, I. Alshibane, L. G. Bloor, B. Rausch, J. S. J. Hargreaves, L. Cronin, *Sustainable Energy Fuels* **2017**, *1*, 1782.
[47] M. Hutin, M. H. Rosnes, D. L. Long, L. Cronin, *Comprehensive Inorganic Chemistry II: From Elements to Applications* (Eds: J. Reedijk, K. Poeppelmeier), Elsevier Ltd., New York **2013**.
[48] E. Papaconstantinou, M. T. Pope, *Inorg. Chem.* **1967**, *6*, 1152.
[49] J. Lei, J.-J. Yang, T. Liu, R.-M. Yuan, D.-R. Deng, M.-S. Zheng, J.-J. Chen, L. Cronin, Q.-F. Dong, *Chem.- Eur. J.* **2019**, *25*, 11432.
[50] J.-J. Chen, M. D. Symes, L. Cronin, *Nat. Chem.* **2018**, *10*, 1042.
[51] V. Amstutz, K. E. Toghill, F. Powlesland, H. Vrubel, C. Comninellis, X. Hu, H. H. Girault, *Energy Environ. Sci.* **2014**, *7*, 2350.
[52] A. Mills, T. Russell, *J. Chem. Soc., Faraday Trans.* **1991**, *87*, 1245.
[53] A. Ho, X. Zhou, L. Han, I. Sullivan, C. Karp, N. S. Lewis, C. Xiang, *ACS Energy Lett.* **2019**, *4*, 968.
[54] C. C. L. McCrory, S. Jung, J. C. Peters, T. F. Jaramillo, *J. Am. Chem. Soc.* **2013**, *135*, 16977.
[55] S. Goodwin, D. A. Walsh, *ACS Appl. Mater. Interfaces* **2017**, *9*, 23654.
[56] W. Li, N. Jiang, B. Hu, X. Liu, F. Song, G. Han, T. J. Jordan, T. B. Hanson, T. L. Liu, Y. Sun, *Chem* **2018**, *4*, 637.
[57] D. E. Green, S. Mii, P. M. Kohout, *J. Biol. Chem.* **1955**, *217*, 551.
[58] D. E. Green, J. Järnefelt, H. D. Tisdale, *Biochim. Biophys. Acta* **1959**, *31*, 34.
[59] F. L. Crane, *Mitochondrion* **2007**, *7*, S2.
[60] K. Saito, A. W. Rutherford, H. Ishikita, *Proc. Natl. Acad. Sci. USA* **2013**, *110*, 954.
[61] B. Rausch, M. D. Symes, L. Cronin, *J. Am. Chem. Soc.* **2013**, *135*, 13656.
[62] N. Kirkaldy, G. Chisholm, J.-J. Chen, L. Cronin, *Chem. Sci.* **2018**, *9*, 1621.
[63] B. Huskinson, M. P. Marshak, C. Suh, S. Er, M. R. Gerhardt, C. J. Galvin, X. Chen, A. Aspuru-Guzik, R. G. Gordon, M. J. Aziz, *Nature* **2014**, *505*, 195.
[64] L. Chen, X. Dong, Y. Wang, Y. Xia, *Nat. Commun.* **2016**, *7*, 11741.
[65] J. Dai, S. F. Y. Li, T. D. Xiao, D. M. Wang, D. E. Reisner, *J. Power Sources* **2000**, *89*, 40.
[66] A. Landman, H. Dotan, G. E. Shter, M. Wullenkord, A. Houaijia, A. Maljusch, G. S. Grader, A. Rothschild, *Nat. Mater.* **2017**, *16*, 646.
[67] J. Jia, L. C. Seitz, J. D. Benck, Y. Huo, Y. Chen, J. W. D. Ng, T. Bilir, J. S. Harris, T. F. Jaramillo, *Nat. Commun.* **2016**, *7*, 13237.
[68] J. Luo, J. H. Im, M. T. Mayer, M. Schreier, M. K. Nazeeruddin, N. G. Park, S. D. Tilley, H. J. Fan, M. Grätzel, *Science* **2014**, *345*, 1593.
[69] C. R. Cox, J. Z. Lee, D. G. Nocera, T. Buonassisi, *Proc. Natl. Acad. Sci. USA* **2014**, *111*, 14057.
[70] M. M. May, H.-J. Lewerenz, D. Lackner, F. Dimroth, T. Hannappel, *Nat. Commun.* **2015**, *6*, 8286.
[71] E. Verlage, S. Hu, R. Liu, R. J. R. Jones, K. Sun, C. Xiang, N. S. Lewis, H. A. Atwater, *Energy Environ. Sci.* **2015**, *8*, 3166.
[72] H. Dotan, A. Landman, S. W. Sheehan, K. D. Malviya, G. E. Shter, D. A. Grave, Z. Arzi, N. Yehudai, M. Halabi, N. Gal, N. Hadari, C. Cohen, A. Rothschild, G. S. Grader, *Nat. Energy* **2019**, *4*, 786.
[73] M. D. Symes, *Nat. Energy* **2019**, *4*, 730.
[74] A. Landman, R. Halabi, P. Dias, H. Dotan, A. Mehlmann, G. E. Shter, M. Halabi, O. Naseraldeen, A. Mendes, G. S. Grader, A. Rothschild, *Joule* **2020**, *4*, 448.
[75] Z. Jin, P. Li, D. Xiao, *ChemSusChem* **2017**, *10*, 483.
[76] B. Choi, D. Panthi, M. Nakoji, T. Kabutomori, K. Tsutsumi, A. Tsutsumi, *Chem. Eng. Sci.* **2017**, *157*, 200.

[77] R. Palumbo, R. B. Diver, C. Larson, E. N. Coker, J. E. Miller, J. Guertin, J. Schoer, M. Meyer, N. P. Siegel, *Chem. Eng. Sci.* **2012**, *84*, 372.
[78] S. Nudehi, C. Larson, W. Prusinski, D. Kotfer, J. Otto, E. Beyers, J. Schoer, R. Palumbo, *Chem. Eng. Sci.* **2018**, *181*, 159.
[79] Y. Ma, X. Dong, Y. Wang, Y. Xia, *Angew. Chem., Int. Ed.* **2018**, *57*, 2904.
[80] J. K. Feng, Y. L. Cao, X. P. Ai, H. X. Yang, *J. Power Sources* **2008**, *177*, 199.
[81] W. Deng, X. Liang, X. Wu, J. Qian, Y. Cao, X. Ai, J. Feng, H. Yang, *Sci. Rep.* **2013**, *3*, 2671.
[82] L. Fan, Q. Liu, Z. Xu, B. Lu, *ACS Energy Lett.* **2017**, *2*, 1614.
[83] Y. Ma, Z. Guo, X. Dong, Y. Wang, Y. Xia, *Angew. Chem., Int. Ed.* **2019**, *58*, 4622.
[84] J. Wang, L. Ji, X. Teng, Y. Liu, L. Guo, Z. Chen, *J. Mater. Chem. A* **2019**, *7*, 13149.
[85] W. Wu, X.-Y. Wu, S.-S. Wang, C.-Z. Lu, *J. Catal.* **2019**, *378*, 376.
[86] C. Ma, S. Pei, S. You, *Electrochem. Commun.* **2019**, *109*, 106611.
[87] L. MacDonald, B. Rausch, M. D. Symes, L. Cronin, *Chem. Commun.* **2018**, *54*, 1093.
[88] S. Lakshmanan, T. Murugesan, *Clean Technol. Environ. Policy* **2014**, *16*, 225.
[89] M. Hou, L. Chen, Z. Guo, X. Dong, Y. Wang, Y. Xia, *Nat. Commun.* **2018**, *9*, 438.
[90] A. Zhao, F. Zhong, X. Feng, W. Chen, X. Ai, H. Yang, Y. Cao, *ACS Appl. Mater. Interfaces* **2019**, *11*, 45126.
[91] A. Landman, G. S. Grader, A. Rothschild, arXiv:2007.13345.

Patrick James McHugh graduated with an M.Sc. in Chemistry from the University of Glasgow in 2018. During his degree, he spent a year on placement at Humboldt-Universität zu Berlin working for Prof. Thomas Braun. Since graduating, Patrick has been pursuing a Ph.D. in Electrochemistry under the supervision of Dr. Mark Symes. In 2019, he was accepted by the European Space Agency as part of a student team to participate in their FlyYourThesis! Programme.

Athanasios D. Stergiou graduated with a B.Sc. in Chemistry from the University of Ioannina in 2016. After obtaining an M.Sc. degree in Green and Sustainable Chemistry from the University of Nottingham (2017), he joined the Symes group at the University of Glasgow to pursue a Ph.D. in electrochemistry. His research interests include indirect electrosynthesis, continuous flow electrochemistry and electrocatalysis.

Mark D. Symes obtained his M.Sc. degree from the University of Cambridge (2005) and a Ph.D. from the University of Edinburgh (2009), before undertaking postdoctoral appointments at the Massachusetts Institute of Technology and the University of Glasgow. He was elevated to the faculty at Glasgow in 2013 and is now a Royal Society University Research Fellow and Senior Lecturer in electrochemistry, electrocatalysis, and electrochemical technology at Glasgow.